THE EFFECTS OF UTILIZING SILICA FUME IN PORTLAND CEMENT PERVIOUS CONCRETE

A THESIS IN
Civil Engineering

Presented to the Faculty of the University
of Missouri-Kansas City in partial fulfillment of
the requirements for the degree

MASTER OF SCIENCE

By
DANIEL ALLEN MANN

B.S. University of Missouri-Kansas City, 2012

Kansas City, Missouri
2014

THE EFFECTS OF UTILIZING SILICA FUME

IN PORTLAND CEMENT PERVIOUS CONCRETE

Daniel Allen Mann, Candidate for the Master of Science Degree

University of Missouri-Kansas City, 2014

ABSTRACT

Silica fume has long been used as a supplementary cementing material to provide a high density, high strength, and durable building material. Silica fume has a particle size a fraction of any conventional cement, which allows it to increase concrete strength by decreasing the porosity especially near the aggregates surface. Because Portland Cement Pervious Concrete (PCPC) has a smaller bond area between aggregate and paste, silica fume has significant impacts on the properties of the PCPC. The research in this paper studies the workability of a cement paste containing silica fume in addition to analyzing the results of testing on Portland Cement Pervious Concrete mixtures that also contained silica fume.

Testing conducted included a study of the effects of silica fume on cement's rheological properties at various dosage rates ranging from zero to ten percent by mass. It was determined that silica fume has negligible effects on the viscosity of cement paste until a dosage rate of five percent, at which point the viscosity increases rapidly.

In addition to the rheological testing of the cement paste, trials were also conducted on the pervious concrete samples. Sample groups included mixes with river gravel and chipped limestone as aggregate, washed and unwashed, and two different void contents.

Workability tests showed that mixtures containing a silica fume dosage rate of 5 percent or less had comparable or slightly improved workability when compared to control groups. Workability was found to decrease at a 7 percent dosage rate. Samples were tested for compressive strength at 7 and 28 days and splitting tensile strength at 28 days. It was found in most sample groups, strength increased with dosage rates of 3 to 5 percent but often decreased when the dosage reached 7 percent. Abrasion testing showed that both samples containing washed aggregate and samples containing silica fume exhibited a reduced mass loss.

APPROVAL PAGE

The faculty listed, appointed by the Dean of the School of Computing and Engineering, have examined a thesis titled "The Effects of Utilizing Silica Fume in Portland Cement Pervious Concrete," presented by Daniel A. Mann, candidate for the Master of Science Degree, and certify in their opinion it is worthy of acceptance.

Supervisory Committee

John T. Kevern, Ph.D., Committee Chair
Department of Civil Engineering

Ceki Halmen, Ph.D.
Department of Civil Engineering

Travis Fields, Ph.D.
Department of Mechanical Engineering

CONTENTS

LIST OF ILLUSTRATIONS

Figure Page

LIST OF TABLES

ACKNOWLEDGEMENTS

The author would like to thank his wife and family for the support and encouragement in addition to their help in editing and proofreading that allowed for the completion of this project. Thanks to Spencer Solon for the assistance in the completion of freeze-thaw testing. A special thanks to Dr. John Kevern for the guidance and insightful direction he was able to give that allowed this research to come to fruition.

CHAPTER 1

INTRODUCTION

In 2013, the American Society of Civil Engineers released its annual "Report Card For America's Infrastructure." With a grade of a "D," wastewater and storm-water management ranks among the most troubling areas; over the next twenty years, the investment needs are approaching $300 billion dollars (American Society of Civil Engineers, 2014). The same study estimates that $64 billion of that total will go towards correcting combined sewer overflow problems. Cities across the United States such as Nashville, Pittsburgh, Seattle, Philadelphia, New York, and Kansas City have been mandated to upgrade their combined sewer systems to prevent combined sewer overflows into local bodies of water. At the same time, cities across the country are struggling to find funding to accomplish this mandate (United States Conference of Mayors, 2005).

For this reason, the need for alternative and cost effective water management solutions is more pressing now than ever. Portland Cement Pervious concrete (PCPC) is one solution recognized by the Environmental Protection Agency (EPA) as a Best Management Practice (BMP) (Enviromental Protection Agency, 2012). PCPC differs from Portland Cement Concrete (PCC) in that in that it allows water to infiltrate through its layers instead of flowing over the surface. PCPC gains this quality through a mix design utilizing an open-graded coarse aggregate and little to no fine aggregate (Wu, Huang, Shu, & Dong, 2011).

While PCPC provides advantages in reducing water runoff, it sacrifices some of the mechanical properties of PCC (Wu, Huang, Shu, & Dong, 2011). PCC gains its strength through a combination of aggregate interlock and bonds from the cement paste. The

reduction of fine aggregates in PCPC yields a substrate bonded primarily by aggregate interlock with little cement paste between. Because of this reduction in paste, raveling and spalling are a constant concern, and are a hindrance in the widespread utilization of PCPC. For this reason, the quality and durability of the cement paste significantly impacts the mechanical properties of PCPC.

This research described in this thesis investigates the effectiveness of using Silica Fume (SF) as a Supplementary Cementitious Material (SCM) in PCPC. SF is a byproduct taken from the arc furnaces in the silicon production industry and exhibits a pozzalonic behavior (Holland, 2005). SF is already used in concrete applications such as bridge decks and shotcrete because of its ability to increase cohesion, compressive strength, and durability.

CHAPTER 2

LITERATURE REVIEW

Silica Fume (SF) is a by-product material from industries which produce silicon containing metals (Federation Internationale de la Precontrainte. Commision on Concrete, 1988). For years, silica fume "smoke" was released into the atmosphere; in the U.S., all SF is now captured to prevent release (Holland, 2005). The SF is captured and collected in the baghouse of silicon arc furnaces and is highly dependent on the amount of silicon produced for other areas of industry (Federation Internationale de la Precontrainte. Commision on Concrete, 1988).

SF is amorphous and has very high silicon dioxide content, in the range of 85 to 98 percent (Holland, 2005). Another significant trait of silica fume is its small particle size, which is as small as 0.1 to 0.2 micrometers. This is much smaller than Ordinary Portland Cement (OPC). In fact, the American Concrete Institute estimates that when OPC is replaced at 15% SF in concrete, there are approximately 2,000,000 grains of SF for every grain of OPC (American Concrete Institute, 1996). SF is fairly uniformly spherical in shape (Holland, 2005). Figure 1 shows a photomicrograph of both OPC and SF at the same magnification. For reference, the longer of the two white bars on the right is 1 micrometer long.

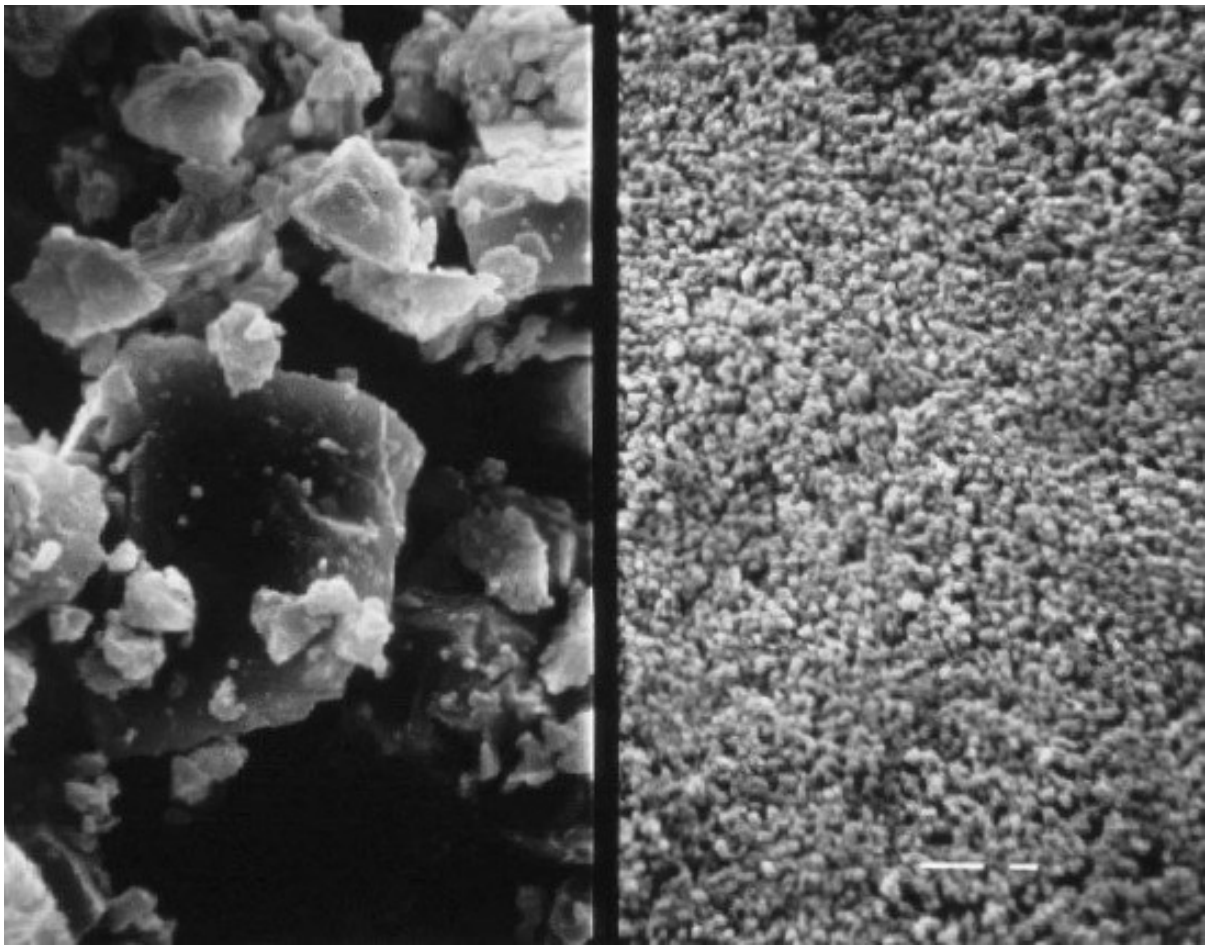

Figure 1 Photomicrograph of OPC (left) and SF (right) at the same magnification **(Holland, 2005)**.

The use of SF has been shown to make chloride and water penetration more difficult (Bohni, 2005). SF is often used in steel reinforced PCC because of its ability to reduce permeability and ability to achieve high strength concrete (McCormac & Brown, 2009). PCC can be easily obtained with compressive strengths up to 12,000 psi using SF with a superplasticizer. SF is also often utilized in PCC mixes to reduce a mixture's susceptibility to abrasion (American Concrete Institute, 1996; Holland, 2005; Rashad, Seleem, & Shaheen,

2014). Silica fume is utilized often in stilling basins on the spillways of dams, loading docks, and other high-load/high-abrasion applications.

Workability has long been known to be affected by the use of SF, often calling for an increase in water demand (Holland, 2005). Although some studies have shown that mineral admixtures such as SF, fly ash, or blast furnace slag actually increase the workability of a cement mixture (Lange, Mortel, & Rudert, 1997), the most typical behavior is that when "volume concentration of solid is held constant, the addition of mineral admixtures improves concrete performance but reduces workability" (Ferraris, Obla, & Hill, 2001).

The study of the rheology is important in cement mixtures since the aggregate in concrete makes true rheology measurements difficult and requiring expensive machinery. While marsh and mini-slump cone tests are often used as an attempt to capture the rheological properties of cement paste, they do not have a significant correlation (Ferraris, Obla, & Hill, 2001). The mini-slump cone attempts to measure the rheological properties by measuring the spread of the paste and the marsh cone attempts this by measuring the time it takes for a given volume of cement to pass through an orifice. Many studies have found that a parallel plate or concentric cylinder rheometer are more accurate and reproducible than the simpler methods (Lu & Wang, 2011; Ferraris, Obla, & Hill, 2001; Vikan, Justnes, Winnefeld, & Figi, 2007).

Rheology is typically measured by viscosity and shear rate. Fluids are typically described as being a Newtonian or non-Newtonian fluid. A Newtonian fluid has a strain rate that is proportional to the shear stress. Conversely, a non-Newtonian fluid has a shear rate that is not proportional to the shear stress. For this reason, often times different models are needed to describe and predict the behavior of different fluids.

Rheological models such as the Power-law, Bingham-Plastic, Herschel-Buckley, Robertson Stiff, Casson, Sisko, Eyring, DeKee, and Vomberg models have been used to model the behaviors of cement (Vikan, Justnes, Winnefeld, & Figi, 2007). These models all attempt to create a model that correlates the shear stress to the shear rate.

The Bingham-Plastic Model is typically applied on viscoplastic materials that behave as a solid when low stresses are applied and as a liquid when high stresses are applied. In simple terms, before a certain threshold of stress is met, the liquid does not flow. According to Bingham's model, once a fluid does meet this threshold stress, its viscosity and shear rate have a linear relationship (Bingham, 1922). The equation for the Bingham model is expressed in terms of:

$$\boldsymbol{\tau = \tau_y + \mu_p \gamma} \quad \textbf{(1)}$$

where:

$\boldsymbol{\tau}$ = shear stress

$\boldsymbol{\tau_y}$=yield stress parameter

$\boldsymbol{\gamma}$ =shear rate

$\boldsymbol{\mu_p}$=plastic viscosity

It can be seen by analyzing the Bingham-Plastic model that the initial yield stress term, $\boldsymbol{\tau_y}$, is simply the amount of stress that must be exerted on the fluid before the fluid begins to move. Another important point to note about the Bingham-Plastic equation is that the derivative of the equation, or the slope of a graph of the equation, is equal to the plastic viscosity, $\boldsymbol{\mu_p}$.

A different model commonly applied to cement rheology was introduced several

years after Bingham revealed his equation (Herschel & Bulkley, 1926). While the Bingham-Plastic model describes fluids relationship between shear stress and shear strain in a neat linear relationship, Herschel-Buckley attempts to describe non-Newtonian fluids often complex relationship between stress and shear. The Herschel-Buckley equation is expressed in terms of:

$$\boldsymbol{\tau = \tau_y + K\gamma^n} \quad (2)$$

where:

K=consistency in Pascal-Seconds to the "nth" power

n=Power Law Index.

The Herschel-Buckley model deviates from the Bingham-Plastic model in that for all Power Law Indices, n, greater than one, the viscosity is dependent on the shear rate. That is, the liquid can be described as having either shear thinning or shear thickening tendencies. Cement has been shown in many studies to exhibit either shear thickening or shear thinning with specific dosage rates of mineral or chemical admixtures (Lootens, Hebraud, Lecolier, & Van Damme, 2004; Vikan, Justnes, Winnefeld, & Figi, 2007) .

One study examined the rheological implications of metakaolin, multiple kinds of fly ash, and SF. One of its conclusions was that for the cement mixtures evaluated, SF had the "worst rheological improvement" (Ferraris, Obla, & Hill, 2001). When SF is used in a cement mixture, it is often practical to compensate for the reduction in workability with a chemical admixture or by modifying the water to cementing materials (W/C) ratio. When SF is used, studies have found that by increasing the dosage of High Range Water Reducer (HRWR), the SF mixture can remain at the same yield stress and viscosity.

While the effects of SF on the workability and rheology can be debated, SF has been

shown to have substantial effects on other properties of concrete. It has been widely recognized that the aggregate-cement paste Interfacial Transition Zone (ITZ) has significant impact on concrete permeability and concrete strength. As shown in Figure 1, SF has a much smaller particle size which allows it to fill in the microstructure deformities that occur in the ITZ (Holland, 2005). For this reason, SF has been shown at certain doses to increase the compressive strength and freeze-thaw resistance of PCC and PCPC (Limbachiya, Meddah, & Ouchagour, 2012; Yang & Jiang, 2003).

Studies have shown that the ITZ has a greater effect on PCPC than PCC (Lian & Zhuge, 2010). The study concludes that in PCPC more fractures developed in the ITZ. Additional findings were that without some sort of filler material such as sand or a chemical admixture, the bond strength was not sufficient between the aggregate and the paste. It went on to state that when the bond was not sufficient, the ITZ became the controlling factor in the compressive strength of the concrete.

The review of the freeze-thaw characteristics of high performance concrete by Aitcin concluded that the addition of silica fume could reduce the chloride ion permeability of concrete to less than 1000 coulombs with a water to cement ratio in the 0.40 to 0.45 range. Although the Rapid Chloride Permeability (RCP) test is not a test that can be conducted on PCPC, it is a test that is conducted on PCC to determine the permeability of the concrete which can then be correlated to concrete's freeze-thaw properties.

The study conducted by Yang and Jiang concluded that it was "difficult to obtain high-strength materials using the common materials and proportion of mixture" (Yang & Jiang, 2003). It went on to suggest different admixtures and aggregate gradations that could be used to increase the mechanical properties of PCPC. One of the focuses of the authors

was the addition of SF and a superplasticizer (SP). In testing the SF in the PCPC, the strength was reduced in the PCPC samples that did not contain some sort of admixture to help allow the SF to equally distribute into the paste. The authors concluded that the addition of these materials could greatly increase the strength of the concrete. Related studies came to similar conclusions (Lian & Zhuge, 2010). The study by Lian and Zhuge concluded that the SF had a positive effect on the compressive strength of the concrete. However, the study also noted that the addition of SF increased the water demand of the concrete mixture. For this reason, the authors concluded that the benefits of SF were not realized unless a chemical admixture was utilized. The use of a superplasticizer allowed for not only improved strength characteristics, but also improved workability.

CHAPTER 3

MATERIALS

Two different types of aggregate were used in the investigation of silica fume. The information on the coarse aggregate is listed in Tables 1 and 2.

Table 1 Limestone Aggregate Information

Property	**Value**
Aggregate	¼ in. Limestone
Specification	ASTM C33
Source	Greenwood Ledge
Specific Gravity (OD)	2.59 (ASTM C127)
Absorption (%)	1.8 (ASTM C127)
Dry Rodded Unit Weight (pcf)	97.0 (ASTM C127_

Table 2 River Gravel Aggregate Information

Property	**Value**
Aggregate	River Gravel
Specification	ASTM C33
Source	Missouri River
Specific Gravity (OD)	2.59 (ASTM C127)
Absorption (%)	0.5 (ASTM C127)
Dry Rodded Unit Weight (pcf)	101.9 (ASTM C127)

The information on the fine aggregate is contained in Table 3. The information on the cement is listed in Table 4. The cement used was from the Lefarge plant located in Sugar Creek, Missouri and met the requirements for both Type I and Type II cement.

Table 3 Fine Aggregate Information

Property	Value
Aggregate	Fine Concrete Sand
Specification	C33
Source	Holiday
SG (OD)	2.64
Abs(%)	0.4

Table 4 Cement Information

Property	Value
Manufacturer	Lafarge
Location	Sugar Creek
Type	I/II Moderate Heat of Hydration
Specific Gravity	3.15

The information on the SF used is listed in Table 5. The SF used in testing was grade 920 undensified SF manufactured by Elkem. Undensified SF typically has a bulk density of between 200 and 350 kg/m^3 where densified SF is in the range of 500 to 700 kg/m^3. The SF used in this testing had a bulk density of just less than 300 kg/m^3 (18.11 lbs/ft^3).

Table 5 Silica Fume Information

Property	Value
Manufacturer	Elkem
Loss On Ignition	3.41%
pH	7.66
Specific Gravity	2.2
Bulk Density (lbs/ft^3)	18.11

The information for the type of High Range Water Reducer (HRWR), Air Entraining Agent (AEA), and Hydration Stabilizer (HS) are listed in table 6. The Gelenium 7500

HRWR is chemical admixture that meets the requirements put forth by ASTM C494 for a Type F HRWR. The BASF MB-VR Standard used in the mixtures is a neutralized vinsol resin type AEA. The Delvo Stabilizer admixture is a chemical that helps control the uniformity and predictability of the hydration of cementitious materials by acting as an ASTM C494 Type B retarding agent.

Table 6 Chemical Admixture Information

Admixture	**Name**
High Range Water Reducer (HRWR)	BASF Glenium 7500
Air Entraining Agent (AEA)	BASF VR Standard
Hydration Stabilizer (HS)	BASF Delvo Stabilizer

CHAPTER 4

MIXTURE PROPORTIONS

During the phases of testing, three different types of mixtures were tested, including paste mixtures, mortar mixtures, and concrete mixtures. The naming convention used for the PCPC mixtures is aggregate "SF dosage – aggregate type – Design Void Content." Mixtures were evaluated for washed and unwashed aggregate states since the cleanliness of aggregate has been known to affect the aggregate bond strength and workability of concrete. Typically aggregates that are especially dirty are not able to bond as securely with the cement paste and often experience durability issues. The aggregates that are not washed are denoted with a "U" preceding the aggregate name. The aggregate names utilized for this mix are listed in table 7.

Table 7 Aggregate Naming Convention

Mixture Name	**Mixture**
LS	Washed Limestone
ULS	Unwashed Limestone
RG	Washed River Gravel
URG	Unwashed River Gravel

The washed limestone and washed river gravel was washed in approximately 50 pound batches in buckets that had holes drilled in the sides of the containers to allow water to drain. When water was applied to the limestone and river gravel, the runoff water was visibly darkened by the chert and sediment that would have passed the #200 seive. The aggregate was washed until the runoff water was visibly clear which usually required

transferring the aggregate between containers to wash out sediment that had settled to the bottom.

The naming convention for the paste mixtures used to evaluate the rheological impacts of adding SF is "P - dosage rate of the SF by percent." In this phase of testing, the only variable changed between mixes was the dosage rate of the SF. The letter "P" denotes that the mixture was a paste only mix. Using the same convention as the paste and concrete mixture, mortars are named "M – dosage rate of the SF by percent."

Paste Mixtures

Dosage rates were investigated ranging from 0% replacement by weight to 10% replacement by weight. Table 8 shows the different paste mixtures analyzed for rheological properties. HRWR dosages were held constant to allow for an accurate comparison between paste mixtures.

Table 8 Paste Mixtures

Mix	Percent SF by Weight	W/C	HRWR (oz/cwt)
P-0	0.0	0.40	1.0
P-1	1.0	0.40	1.0
P-2	2.0	0.40	1.0
P-3	3.0	0.40	1.0
P-4	4.0	0.40	1.0
P-4.5	4.5	0.40	1.0
P-5	5.0	0.40	1.0
P-5.5	5.5	0.40	1.0
P-6	6.0	0.40	1.0
P-7	7.0	0.40	1.0
P-8	8.0	0.40	1.0
P-9	9.0	0.40	1.0
P-10	10.0	0.40	1.0

Mortar Mixtures

Only one mixture proportion was created to analyze the effects of ultrasound on particle distribution and compressive strength, but these same mixture proportions were mixed under different conditions. The mix utilized the mixture proportions found in ASTM C109 using 2.75 standard sand to cementitious materials ratio and a 5 percent SF replacement by mass. The mixture utilized a 0.40 water to cementitious materials ratio and a dosage of 5 oz/cwt of HRWR.

Pervious Concrete Mixtures

While the initial phase of testing was to investigate a PCPC mixture with 25% voids with an OPC replacement rate of 5% by weight, testing results dictated that other mixes be evaluated. Table 9 shows the mix design for PCPC utilizing limestone CA with a 5% SF replacement.

Table 9 Pervious Concrete Mixes Designed for 25% Voids with Limestone

Mixture	0 - LS - 25	5 - LS - 25	0 - ULS - 25	5 - ULS - 25
W/C	0.32	0.32	0.32	0.32
PC (lb)	563	535	563	535
SF (lb)	0	28	0	28
CA (lb)	2182	2172	2182	2172
FA (lb)	164	164	164	164
AEA (oz/cwt)	1	1	1	1
HS (oz/cwt)	4	4	4	4
HRWR (oz/cwt)	5	5	5	5

Limestone was also investigated at a 20% void rate. In contrast to the initial mixture, this limestone mixture was evaluated at 0, 3, 5, and 7 percent cement replacement rates. Table 10 and 11 show the mix designs for the washed and unwashed limestone respectively.

Table 10 Pervious Concrete Mixes Designed for 20% Voids with Washed Limestone

Mixture	0 - LS - 20	3 - LS - 20	5 - LS - 20	7 - LS - 20
W/C	0.32	0.32	0.32	0.32
PC (lb/yd^3)	601	582	570	559
SF (lb/yd^3)	0	18	30	42
CA (lb/yd^3)	2327	2321	2317	2313
FA (lb/yd^3)	175	175	174	174
AEA (oz/cwt)	1	1	1	1
HS (oz/cwt)	4	4	4	4
HRWR (oz/cwt)	5	5	5	5

Table 11 Pervious Concrete Mixes Designed for 20% Voids with Unwashed Limestone

Mixture	0 - ULS - 20	3 - ULS - 20	5 - ULS - 20	7 - ULS - 20
W/C	0.32	0.32	0.32	0.32
PC (lb/yd^3)	601	582	570	559
SF (lb/yd^3)	0	18	30	42
CA (lb/yd^3)	2327	2321	2317	2313
FA (lb/yd^3)	175	175	174	174
AEA (oz/cwt)	1	1	1	1
HS (oz/cwt)	4	4	4	4
HRWR (oz/cwt)	5	5	5	5

In addition to evaluating mixes utilizing limestone, mixes were also evaluated utilizing a smooth river gravel. Similar to the limestone mixtures, the river gravel was also evaluated in a washed and unwashed state. Mix designs for the washed and unwashed river

gravel is shown in tables 12 and 13 respectively. Mixes were conducted with similar dosages of chemical admixtures to allow for a better comparison of workability.

Table 12 Pervious Concrete Mixes Designed for 20% Voids with River Gravel

Mixture	0 - RG - 20	3 - RG - 20	5 - RG - 20	7 - RG - 20
W/C	0.32	0.32	0.32	0.32
PC (lb)	601	582	571	559
SF (lb)	0	18	30	42
CA (lb)	2327	2321	2318	2313
FA (lb)	175	175	175	174
AEA (oz/cwt)	1	1	1	1
HS (oz/cwt)	4	4	4	4
HRWR (oz/cwt)	5	5	5	5

Table 13 Pervious Concrete Mixes Designed for 20% Voids with Unwashed River Gravel

Mixture	0 - URG - 20	3 - URG - 20	5 - URG - 20	7 - URG - 20
W/C	0.32	0.32	0.32	0.32
PC (lb)	601	582	571	559
SF (lb)	0	18	30	42
CA (lb)	2327	2321	2318	2313
FA (lb)	175	175	175	174
AEA (oz/cwt)	1	1	1	1
HS (oz/cwt)	4	4	4	4
HRWR (oz/cwt)	5	5	5	5

CHAPTER 5

MIXING METHODS

Because of the importance of the distribution of SF in the cement paste, increased emphasis was placed on mixing techniques used with SF mixtures. The unique properties of SF called for differing mixing techniques depending on the type of mixture being evaluated and the type of testing being conducted.

Paste Mixture Methods

Before adding any material to the Hobart mixer, the HRWR was measured and added to the water container containing the previously measured water quantity. The SF was also measured and briefly mixed with a spoon with the dry OPC. The water and HRWR were added to the mixing bowl first, and the SF and Cement added and allowed to absorb into the water for approximately 30 seconds according to ASTM C305. The mixer was then started and mixed for 30 seconds. The mixer was then stopped to scrape the sides and the wire whisk paddle for approximately 15 seconds. The mixer was then restarted at medium speed for the remaining 60 seconds. The "zero" minute mark, for the purposes of this testing, was the end of the mixing time specified for cement pastes by ASTM. In other words, if a mix says it was mixed for 10 minutes, it means it was mixed for 10 minutes in addition to the ASTM C305 mixing time.

Initially, the P – 5 mixture was evaluated to determine the best mixing paddle. Then it was tested at various times, up to 90 minutes, to evaluate the correct mixing time. The paste mixes were mixed in a Hobart Mixer utilizing a whisk style paddle. The whisk style paddle was determined as a best fit for mixing in preliminary stages of testing as it appeared to shear

the paste more than the other paddles. It was determined that a total mixing time of 10 minutes was appropriate with the given mix design. The rheology testing that led to these results is discussed in more detail in Chapter 7 of this paper.

The P-5 and P-0 mixtures were also evaluated for their performance in hot weather conditions. For this phase of testing, the mixtures were mixed for 90 minutes at 90 degrees Fahrenheit plus or minus 1 degree and around 20 percent humidity. The mixture was evaluated for rheological properties every 10 minutes. Figure 2 shows the mixer inside the oven subsequent to a round of testing.

Figure 2 Hot Weather Mixing Configuration

Mortar Mix Method

Several studies have utilized Ultrasound to disperse the flocculated SF particles before mixing a mortar or concrete (Vikan, Justnes, Winnefeld, & Figi, 2007). This research attempted to evaluate the effectiveness of using ultrasound during the mixing process. Mortar was mixed by hand inside a metallic bowl inside the ultrasound cleaning bath shown in Figure 3 using a metal spoon. The Crest CP500HT Ultrasonic Heated Cleaner had an ultrasonic frequency of 45 kHz. Although adjustments had to be made because of the differing mixing equipment, an attempt was made to adapt ASTM C305 instructions to the hand mixing method. All of the mixing water and HRWR was added to the mixing pan. The cement was then added to the water and mixed for approximately 60 seconds. The sand was then mixed in over a 60 second period, followed by 2 minutes of vigorous mixing. The mixture was allowed to rest, followed by an additional 2 minutes of hand mixing.

Figure 3 Mortar Ultrasound Mixing

Pervious Mix Method

The PCPC was mixed according to ASTM Standard C192. When mixing PCPC, it is imperative to observe the workability of the mix. PCPC is more sensitive than PCC in that if the measured moisture content of the aggregate used in the mix deviates by a small amount, the mixture can be wet enough the voids on the surface close yielding a PCPC sample with little to no drainable properties. Figure 4 shows a picture of a mix that had too much bleed water that would have reduced the permeability of the sample. This sample was not used in any testing.

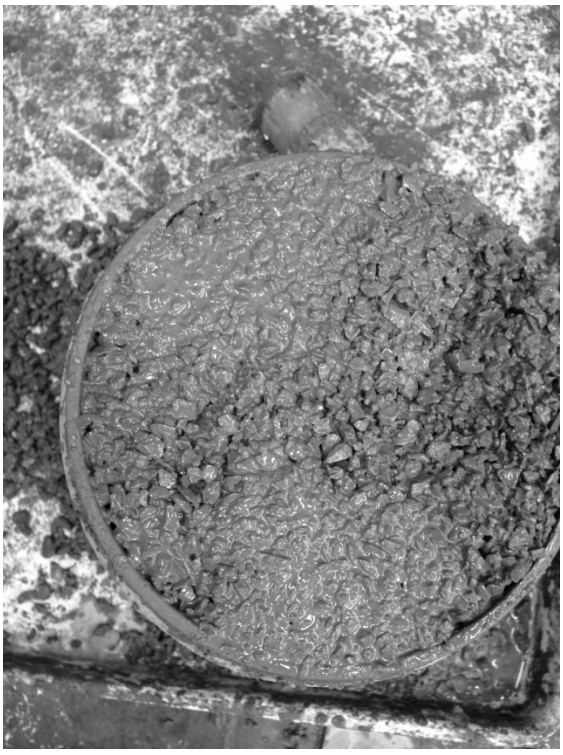

Figure 4 PCPC Sample with Too Much Water Added

CHAPTER 6

TEST METHODS

All tests were conducted in triplicate unless otherwise stated and the analysis of the results was done using a student t test assuming a normal distribution and α=.05.

Paste Testing

Rheology testing was conducted using a Brookfield Viscometer model RVDV-II+P. The Brookfield Rheometer is a concentric cylinder rheometer that measures the shear stress at various shear rates. Figure 5 shows an image of the viscometer used for the experimentation.

Figure 5 Brookfield Viscometer Model Used for Testing

Figure 6 shows the spindle and paste capsule used to test the rheological properties of the paste. The cement paste mixture was mixed in the manner described in the previous section and immediately filled to approximately the halfway point on in the capsule. The spindle was then inserted, and any overflow paste wiped away.

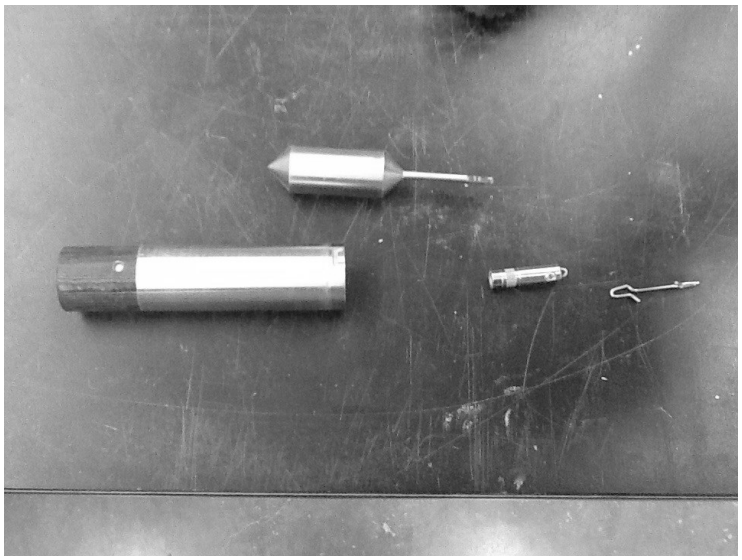

Figure 6 Capsule and Spindle of Brookfield Viscometer

After the spindle assembly was in place, it was attached to the viscometer and a program was started to begin measuring the rheological properties. The program used was such that the shear rate was varied from 1 sec^{-1} to 50 sec^{-1} and back to 1 sec^{-1}. It was found that consistently error was observed in the measurement of the shear stress at low shear rates as the spindle was just starting to move. For this reason, the yield stress and viscosity were evaluated on the return slope of the cycle. The total testing length took approximately 120 seconds to complete.

In an attempt to find the paste mixture with the greatest SF dosage before rheological properties begin to degrade, it was imperative to find the mixing time at which point the mix

was homogeneous and the HRWR had taken effect. In order to achieve this, the mixture was tested at intervals ranging from 0 to 90 minutes. During this testing, the mixer was stopped just long enough to remove a sample, then returned to mixing.

Based on the first phase of rheology testing, it was determined the mixing time would be 10 minutes for the paste mixture. Further discussion of this conclusion is located in the Results and Discussion portion of this paper.

The second phase of this test consisted of varying the amount of SF in the cement paste to determine the exact amount of SF that would result in the most workable mixture. Initially it was determined that a handful of dosage rates between 0% and 15% would be tested. Upon testing, it became apparent that significantly more trials were needed to adequately describe the impacts that the SF had on the paste. For this reason, the testing was conducted on every integral percentage from 0% to 10%. Testing was cut off at 10% because the rheological impacts of the SF did not allow the viscometer to test above this range.

Mortar Testing

Mortar samples were tested for compressive strength after 7 days. All of the cubes were tested according to American Society for Testing and Materials (ASTM) C109 (ASTM Standard C109, 2013). Figure 7 shows the test setup for the compressive strength testing for the mortar cubes.

Figure 7 ASTM C109 Mortar Cube Compressive Strength Testing

Pervious Testing

There were multiple standard ASTM tests conducted on the pervious concrete mixtures. These tests are listed in Table 14. The testing equipment used to perform these tests are calibrated to the ASTM specified standards.

Table 14 ASTM Standard Testing Conducted on Pervious Mixtures

Test	ASTM Standard
Compressive Strength	C39 (ASTM Standard C39, 2005)
Splitting Tensile Strength	C496 (ASTM Standard C496, 2004)
Rotary Abrasion	C944 (ASTM Standard C944, 1999)
Impact Abrasion	C1747 (ASTM Standard C1747, 2011)
Hardened Density and Voids	C1754 (ASTM Standard C1754, 2012)
Freeze/Thaw	C666 (ASTM Standard C666, 2008)

Compressive strength testing was conducted on every sample listed in the previous section (ASTM Standard C39, 2005). All samples were sulfur-capped as called for in the testing standard. Figure 8 shows a picture of the capping-capping process and Figure 9 shows the capped-capped sample undergoing the compressive strength testing per ASTM C39 test standard.

Figure 8 Capping-Capping Process for Compressive Strength Testing

Figure 9 Compressive Strength Testing of a Pervious Concrete Sample.

In addition to compressive strength testing, splitting tensile testing was conducted according to ASTM C496. In this standard, the cylindrical specimen is placed on its side and crushed with a "diametrical force" until failure (ASTM Standard C496, 2004). Instead of the previously described testing according to ASTM C39, by applying the load in this manner the specimen experiences tensile stresses in the direction containing the load. This test is especially useful since concrete pavement rarely experiences a crushing force equaling that

of a concretes compressive strength. Pavement fails when a void develops under the slab, and the pavement fails in a similar failure mode as does the specimen in this test. Figure 10 shows a sample undergoing ASTM C496.

Figure 10 Splitting Tensile Strength Setup

Two different types of abrasion were conducted on the samples. Rotary abrasion was conducted using ASTM C944. In this test, a PCPC sample was placed in a pan and compacted to the same density as the other samples (ASTM Standard C944, 1999). After curing, the samples were taken out and placed under a modified drill press. The machine used for this phase of testing is shown in Figure 11. Figures 12 and 13 show a before and after of the 0-LS-25 sample

Figure 11 ASTM C944 Rotary Abrasion Apparatus

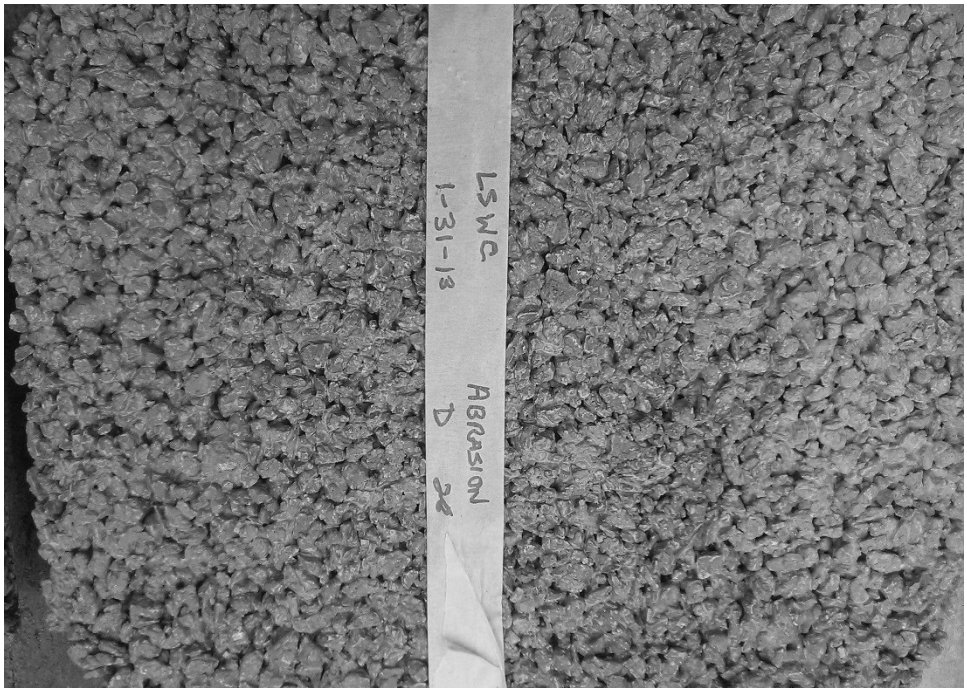

Figure 12 Abrasion Plate Specimen Before Rotary Abrasion Testing

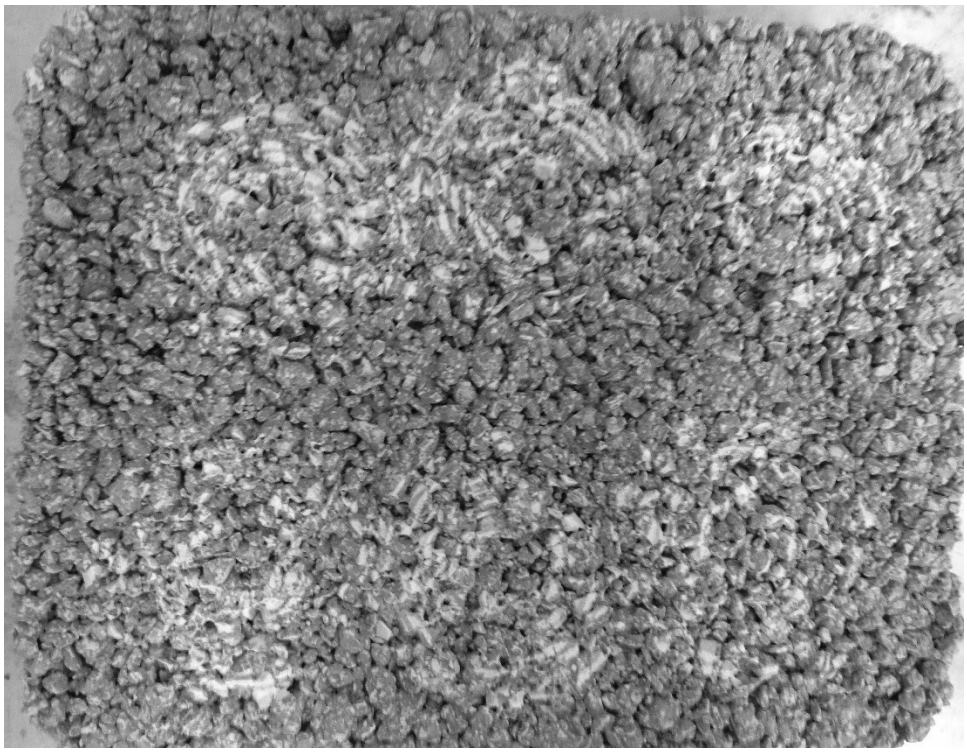

Figure 13 Abrasion Plate Specimen After Rotary Abrasion Testing

The other type of abrasion utilized for testing was impact abrasion. The testing method utilizes an LA Abrasion machine, which consists of a rotating steel drum with a rail on the inside of the drum. In the LA Abrasion test designed for aggregates, steel ball bearings are placed in the rotating drum with the aggregate to aid in the acceleration of their degradation. ASTM C1747 specifies that for PCPC testing, no ball bearings are to be placed in the drum (ASTM Standard C1747, 2011). Instead, three 4 in. diameter by 4 in. tall cylinders were placed at the design void content and tested after curing in sealed conditions. The cylinders were left in the drum for a total of 500 revolutions. The total mass loss was measured after 500 revolutions. It is expected that for more durable mixes the sample may turn into a spherical shape, and for a less durable design may degrade completely into individual aggregate pieces.

Permeability was conducted loosely according to the testing specified in ACI 522R and in the ACI student competition. This test method utilizes a falling head permeameter setup designed specifically for the 4" diameter PCPC specimens used. First, approximately 1" was cut off the top and bottom of the samples to gain a true test of the PCPC's permeability since often times the surface and bottom of the sample are slightly less permeable than the rest of the sample because of compaction. After trimming the sample, the cylinders were wrapped in a plastic shrink wrap with O-ring type seals on each end to ensure the water flowed through and not around the outside edges of the samples. The samples were then placed in the apparatus that contained a rubber sleeve that formed to the outside of the sample. Water was filled to the 9" mark of the water reservoir and drained until it met the 1" mark. The time measured for this to happen was used to calculate the drainage coefficient of the sample that is given in centimeters per second (cm/s). To ensure the sample had no air

voids during the beginning of testing, water was initially run through the sample then refilled to the 9" mark to begin testing.

Calculations were conducted using the following equation:

$$k = \frac{A_1 L}{A_2 t} \ln\left(\frac{h_0}{h_1}\right) \quad (3)$$

where:

k=Coefficient of permeability (cm/sec)

A_1 = Cross Sectional Area of water reservoir

L = Length of the Sample

A_2 = Area of PCPC Sample

t = time to train the reservoir from 9" to 1"

h_0 = Initial height of water

h_1 = Final height of water

The length of the sample was approximately 6" for all specimens and the area just over 12.5 inches^2. Figure 14 shows the testing setup for the falling head permeameter and Figure 15 shows the cut and shrink wrapped samples used for testing.

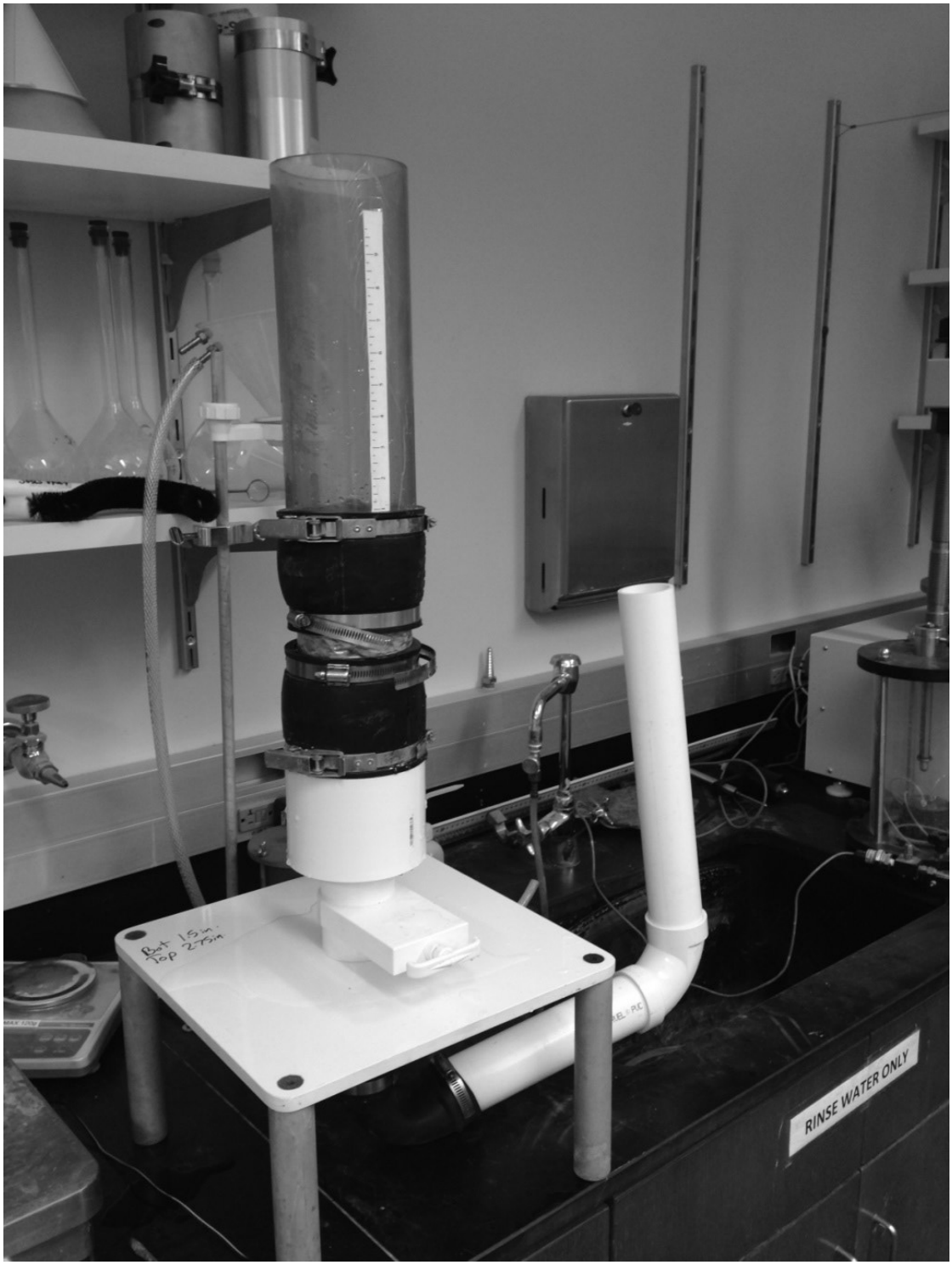

Figure 14 Pervious Concrete Permeability Test Setup

Figure 15 Pervious Concrete Permeability Test Samples

CHAPTER 7

RESULTS AND DISCUSSION

Paste Results

In the rheological phase of the testing, an attempt was made to optimize the workability of a mix design containing SF by testing different dosages as described in Chapter 6. As mentioned earlier, it was first necessary to calibrate the test in order to find the mixing time when the HRWR has taken effect and the SF dispersed.

Figures 16 and 17 illustrate the way that results were measured for the rheological tests. Figure 16 shows the P-5 sample at 10 minutes mixing time. The figure displays the increasing shear rate and the decreasing shear rate for the sample, otherwise known as the hysteresis loop. It was found that with the Brookfield Rheometer, more accurate and smoothed results were observed on the curve measured as the shear was decreasing on the the down curve. For this reason, all calculations were based on the down curve measurement.

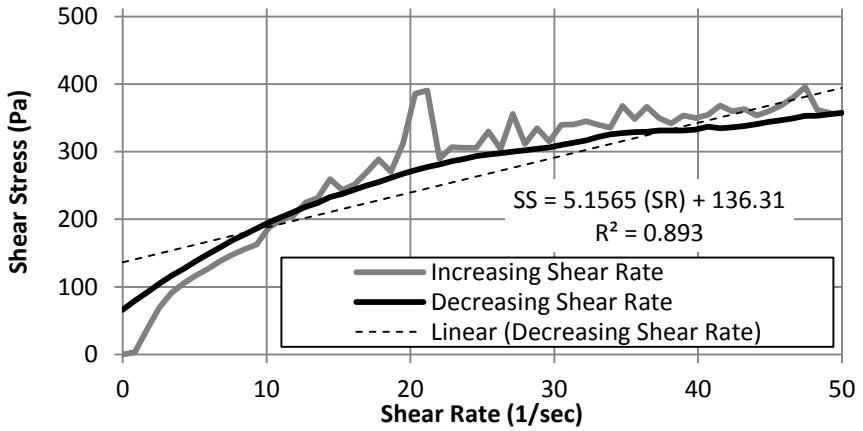

Figure 16 Data Processing for P-5 at 10 Minutes Mixing Time Using Linear Viscosity Model

In Figure 16, a linear regression was used to approximate the best fit line for the entire test at all shear rates. This shows a general representation of the viscosity, but fails to show the higher viscosities at low shear rates that taper off as the shear rate increases. It also fails to adequately show the yield stress of the paste. As explained in the literature review, the yield stress can be found graphically by determining the shear stress when the shear rate is at zero. As can be seen, the Bingham-Plastic best-fit model in this circumstance shows the paste having a yield stress of 136 Pa, when in actuality the paste had a yield stress of just over 66 Pa.

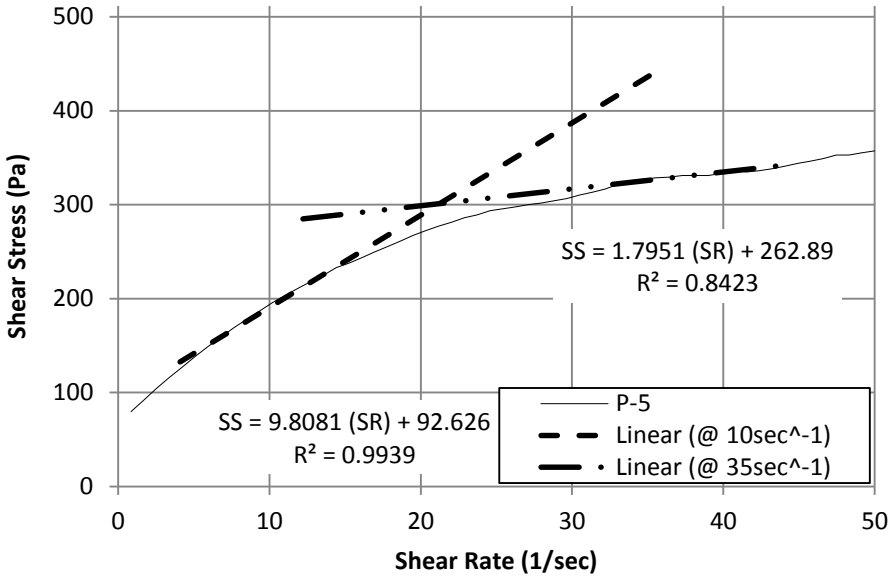

Figure 17 Example of Data Processing for P-5 at 10 Minutes Mixing Time Acknowledging Shear Thinning Behavior

Figure 17 shows the best fit lines for the 10 measurements nearest to the 10 sec^{-1} and 35 sec^{-1} marks. This method of finding the shear rates allows for the idea of a change of shear rate.

Using Sum of Squares model fitting procedure, the Herschel-Buckley model was determined from 3 tests of the P-5 mixture at 10 minutes mixing time. This model is shown in Figure 18 along with the Bingham Plastic Model. The equation derived for the Bingham Plastic model is $\tau = 136.31 + 5.16\gamma$ with a coefficient of determination of 0.89 and the equation derived for the Herschel-Buckley model is $\tau = 32.60 + 59.14\gamma^{0.446}$ with a coefficient of determination of 0.98. To further illustrate the shear thinning behavior of SF in the cement paste, Figure 19 shows the rheological testing results for the control mixture P-0. It should be noted that the Bingham-Plastic model has a coefficient of determination of 0.997 on the sample P-0 shown in Figure 18. This illustrates that for low dosages of SF, the paste follows the Bingham-Plastic model.

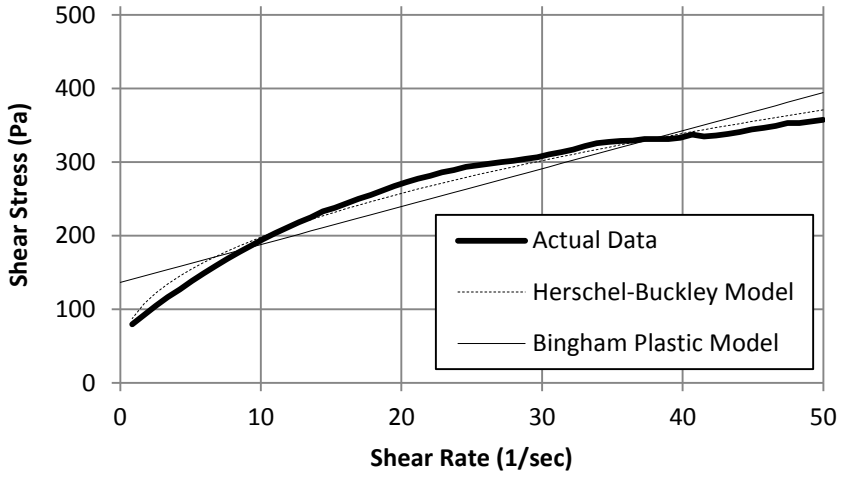

Figure 18 Sum of Squares Model Fitting for Bingham Plastic and Hershell-Bulkley for P-5

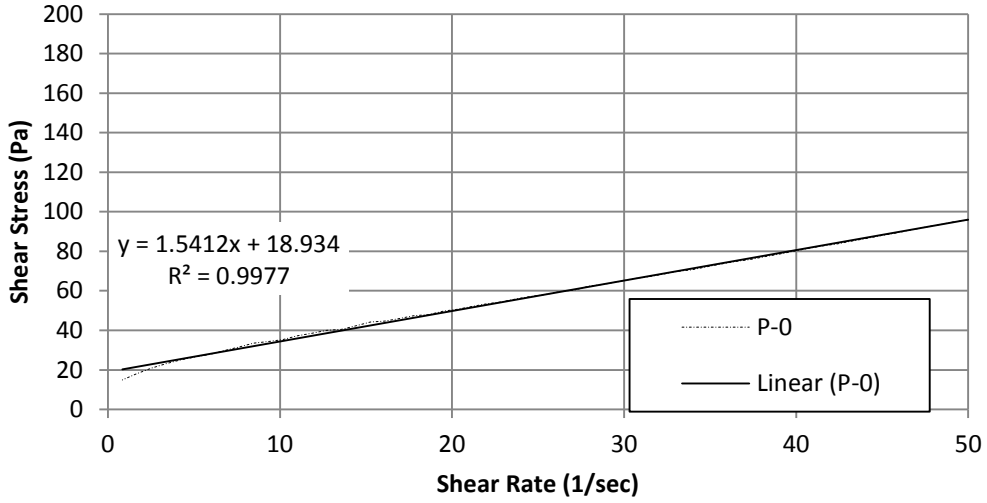

Figure 19 Data Sample Showing Linear Viscosity at 0% SF Dosage

Although it can be seen that the Herschel-Buckley model more accurately describes the rheology behaviors of mixtures with high SF contents, the Bingham Plastic model is typically used in the concrete industry to report viscosities and yield stresses. This is done for several reasons. Since the Herschel-Buckley model does not provide for a constant viscosity value, the Bingham Plastic method is effective in taking an average of the paste behaviors at a range of shear rates. For this reason, the Bingham Plastic model was utilized in the reporting of results for varying SF dosage rates.

Figure 20 shows the data depicting the viscosity and shear stress at times ranging from zero to 90 minutes assuming the Bingham plastic model. As described in the literature review, the Bingham-Plastic model is such that once a liquid reaches a certain shear stress, its relationship between shear stress and shear rate is linear. Thus, the viscosity would be a constant for all shear rates. It should be noted that as described in Chapter 5, the "zero" minute mark corresponds to the amount of mixing time specified for cement paste in ASTM C305.

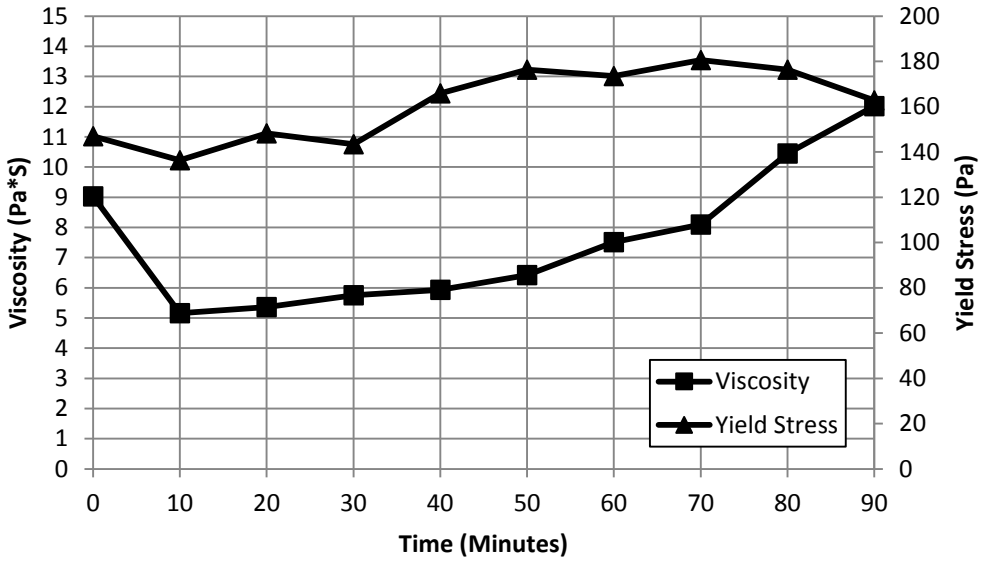

Figure 20 Rheology Results for P-5 at 0 to 90 Minutes Assuming Linear Viscosity

Although Figure 20 shows the rheological properties of cement paste for the determination of mixing times, it should be noted that it neglects the shear thinning behaviors that SF exhibited and are displayed in Figures 17 and 18. This means that, although the Bingham-Plastic model is the most convenient and compact model for viscosity, it does not address the fact that at different shear rates the paste has a different viscosity values. Figure 21 shows the same test data as Figure 20, except viscosity values are shown for two selected shear rates of 10 sec^{-1} and 35 sec^{-1} instead of a constant value. This method of describing the viscosity is similar to the method shown previously in Figure 17.

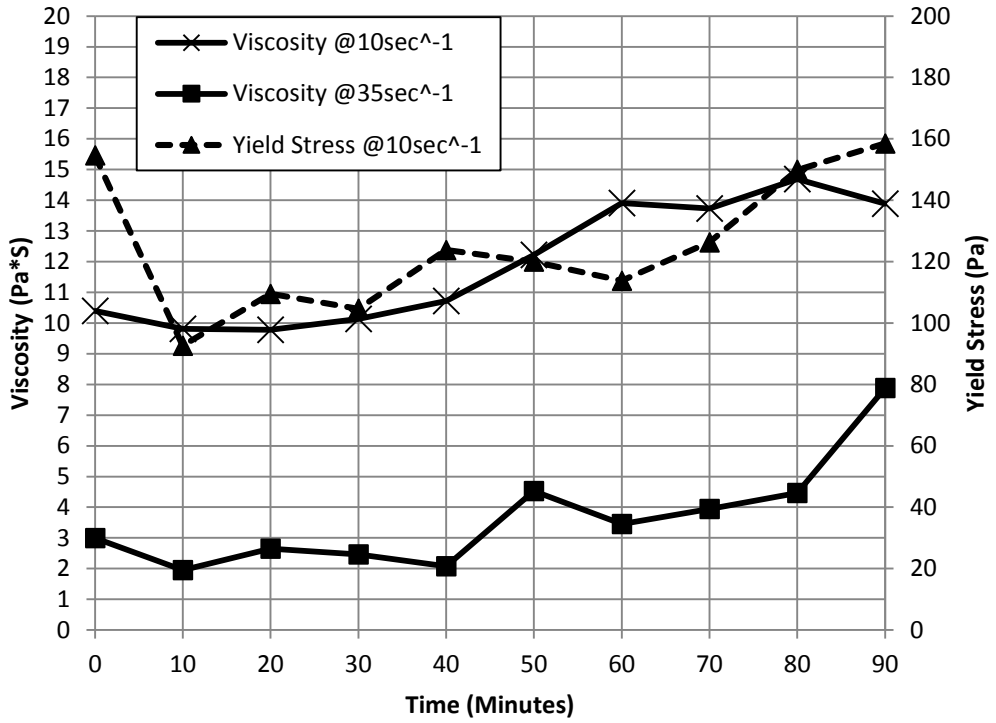

Figure 21 Rheology Results for P-5 at 0 to 90 Minutes at Shear Rates of 10 sec^{-1} and 35 sec^{-1}

Using Figures 20 and 21, it was determined that a mixing time of 10 minutes was optimal. Although more test could have been conducted at increments between 0 and 10 minutes, the duration of each test along with guidance from literature reinforces the conclusion of a 10 minute mixing time (Holland, 2005). Regardless of the assumption that the viscosity is a constant value at any shear rate, the lowest viscosity and yield stress value came at 10 minutes from the completion of ASTM C305 mixing. For this reason, all of the rheological testing conducted for the determination of optimum dosage rate was conducted at a mix time of 10 minutes.

In the next phase of rheology testing the samples were tested with varying dosage rates at 10 minutes mixing time. Figure 22 shows the results of dosage rates ranging from 0 to 10 percent. It was determined through the previous phase of testing that the Bingham

Plastic model would be used for reporting values of viscosity and yield stress for each of the dosage rates. Although the yield stress and viscosity may be different than that of the better fitting Herschel-Buckley model, it was found that it gave a good overall picture of the mixture while reporting a single viscosity value.

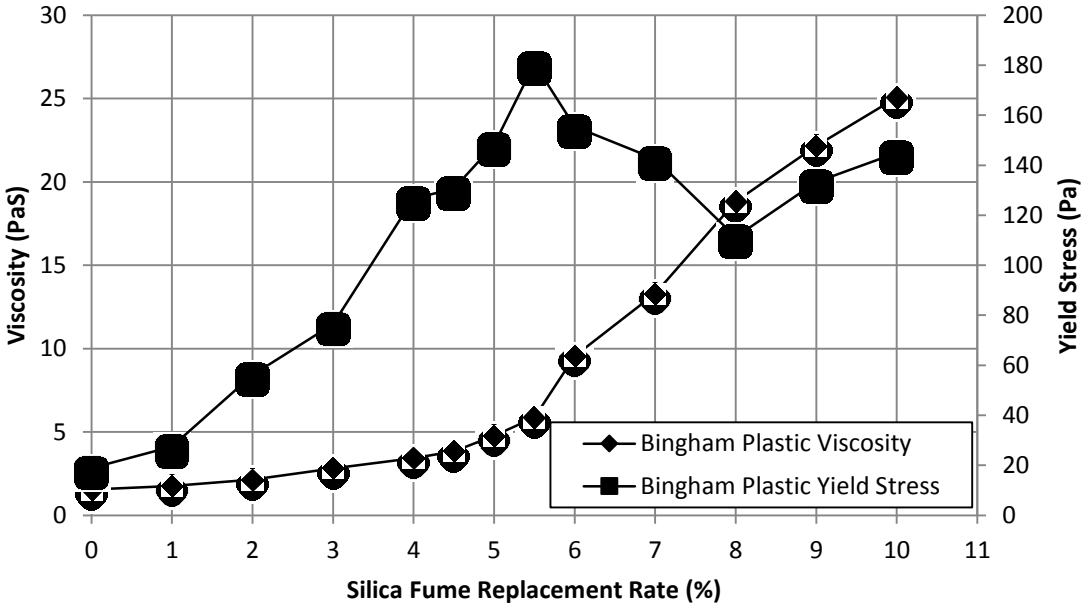

Figure 22 Viscosity and Yield Stress for Different SF Dosage Rates

In evaluating the rheological properties for different dosage rates, it was determined a dosage rate of 5.5 percent SF was the optimum dosage rate for the paste mixtures. As shown in Figure 22, for dosage rates greater than 5.5 percent the viscosity begins to increase quickly. With the knowledge of how concrete mixtures are batched in the field, a SF dosage rate of 5 percent was chosen as the theoretical optimal dosage rate for PCPC.

To determine the effects SF has on hot weather mixing, the rheological properties were investigated using the procedure described in Chapter 5, and the mixing was conducted

in an oven held at a constant temperature of 90 degrees Fahrenheit. The P-0 and P-5 mixtures were evaluated in these conditions. The results of this testing is shown in Figure 23.

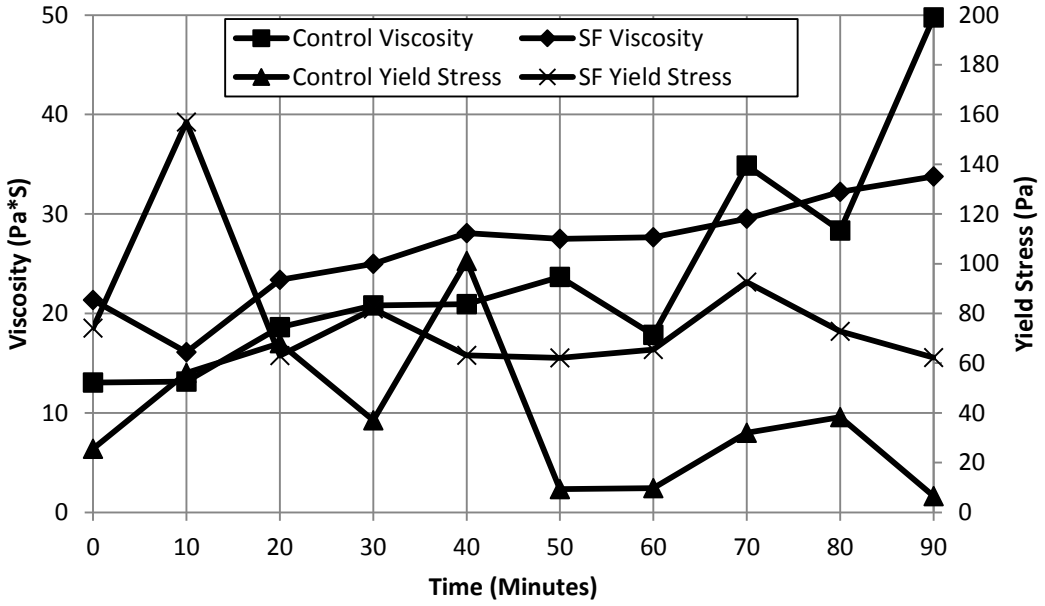

Figure 23 Hot Weather Mixing Rheology

Figure 23 shows several trends exhibited for mixes that contain SF. As expected, the SF sample had a slightly higher initial viscosity. As time passed under hot weather mixing conditions, the viscosity of both mixtures increased. The mixture containing SF increased at a slower rate than the control mixture. It was also apparent in both the rheology results and visually that the SF mixture remained more homogeneous than did the control. As time passed, the control mixture began setting, resulting in peaks and inconsistencies in viscosity measurements.

Mortar Cubes

As described in Chapter 5, a hand mixed mortar with a 5 percent dosage rate was evaluated for the effects that ultrasound would have on the particle dispersion and the compressive strength. The results of the testing showed that the cubes had an average compressive strength of 6710 psi with a Coefficient of Variation (COV) of 18.7 percent when mixed by hand with no ultrasound for the three samples. The COV is defined as the ratio of the standard deviation to the mean and shows the variability in relation to the average value of a sample group. One sample broke at a significantly lower strength than the other two, and if that specimen was assumed to be an outlier, the average for the samples without ultrasound applied during mixing was 7434 psi with a COV of 0.34 percent. When ultrasound was applied to the mixture, the cubes had an average compressive strength of 7149 with a COV of 2.5 percent. Figure 24 shows a typical mortar cube sample after testing.

Figure 24 Typical Mortar Cube Failure

With the given mixture, it appeared that the ultrasound did not increase the compressive strength. It is possible that if a mixture's proportions were reconfigured to make a more workable mix, it could allow for a greater dispersion off the particles during the mixing process. In addition, a configuration that allowed mixing with the standard Hobart mixer while treating the samples with ultrasound could have also increased the effectiveness of the ultrasound at dispersing the flocculated SF particles.

Pervious Concrete

The mixtures described in Chapter 4 were designed, mixed, and placed in a methodology attempting to keep a certain void content. Many PCPC studies attempt to study a variety of mixes, while keeping the compaction effort constant. To provide consistent and reliable testing results, a calibration was performed to determine the mass of PCPC that should be batched in each mold. This is done in order to achieve a specific void content and the compaction effort must be adjusted accordingly. The unit weight of the sample was taken separately according to ASTM C1688 to determine workability. The results of the hardened density test which was conducted in triplicate for all samples is shown in Table 15.

Table 15 Hardened Void Content by ASTM C1754

Mix Design	Void Content (%)	COV (%)
0-LS-25	26.3	1.1
5-LS-25	26.5	1.6
0-ULS-25	26.7	2.5
5-ULS-25	26.6	3.4
0-LS-20	21.0	2.3
3-LS-20	19.6	0.1
5-LS-20	21.1	1.3
7-LS-20	20.5	1.2
0-ULS-20	21.2	1.5
3-ULS-20	20.1	7.1
5-ULS-20	21.3	0.2
7-ULS-20	21.1	4.8
0-RG-20	20.1	1.2
3-RG-20	20.4	6.1
5-RG-20	20.4	2.5
7-RG-20	20.3	1.1
0-URG-20	20.9	1.7
3-URG-20	21.9	0.5
5-URG-20	21.2	1.7
7-URG-20	21.4	1.1

All mixes average values were within 1.9% of the targeted value of 20% or 25%. The mix that was the furthest from the target was the 3-ULS-20, which had a COV of 0.46%. According to ASTM C1754, the single operator COV for a sample is 5.46 using drying method B. Using Analysis of Variance (ANOVA) on the samples, it was determined that they all were statistically similar to their design void contents. The 25% void mixtures had a p-value of 0.88 and F-value of 0.22, which both indicate that the samples are statistically similar. Another ANOVA analysis was also conducted on the samples including a sample group with a mean of 25% and a variance of 1.365. This corresponds to the single operator COV specified in ASTM C1754, and a sample size of 3 which is also specified in the

standard. Using this as the fifth sample group, a p-value was calculated of 0.1525 and an F-value of 2.12.This indicates there is no statistical difference between the actual samples measured and a theoretical 25% average void content sample group.

The LS-20, ULS-20, RG-20, and URG-20 samples were also compared using a similar methodology. The LS-20 and ULS-20 samples had a p-value of 0.058 and an f-value of 2.538, which indicates they are statistically similar. In a similar fashion as described above, in an attempt to validate calling this the 20% void sample group, a theoretical 20% sample group was added to the analysis with a sample size of 3 and single operator COV of 5.46%. The results of this ANOVA test was a p-value of 0.079 and a f-value of 2.20 indicating the samples are statistically similar to the theoretical 20% samples.

The RG-20 samples had a p-value of 0.968 and an f-value of 0.083, which would indicate the RG-20 sample group's voids were statistically similar. The RG-20 and URG-20 samples had a p-value of 0.007 and f-value of 4.398. Although this would normally indicate that the sample groups varied, the low p-value is due to the small sample size. The average values are just over 1 percent different, but the COV for several of the URG-20 samples was extremely small. Time constraints only allowed for 3 samples to be tested for each sample group, but it is expected that if more samples were tested the COV would increase to a COV closer to the 5.46 percent called out in ASTM C1754.

It should be noted that in Table 15, the coefficient of variance (COV) percent given is not the same percent measure as the percent voids of the mixture, but a measure representing the variation in the data. In other words, for mix 3-ULS-20, the actual test values ranged from 18.63% to 21.47%. The COV represents the possible variation as a percent of the measured value.

Permeability testing was also conducted to validate the conclusion that the mixes were the same void content and also to ensure that the mix design was still a drainable mix. The results showed that no trends were apparent when comparing results within aggregate groups, but the permeability differed when comparing between aggregate groups. The river gravel tended to have a higher permeability than did the limestone sample groups. The results of this testing is shown in Table 16.

Table 16 Permeability Results

Mix Design	Permeability (cm/sec)	COV (%)
0-LS-20	0.121	9.6%
3-LS-20	0.103	17.0%
5-LS-20	0.115	21.7%
7-LS-20	0.106	6.9%
0-ULS-20	0.138	6.3%
3-ULS-20	0.117	23.8%
5-ULS-20	0.078	12.1%
7-ULS-20	0.093	8.4%
0-RG-20	0.177	10.2%
3-RG-20	0.149	2.6%
5-RG-20	0.188	4.4%
7-RG-20	0.184	5.0%
0-URG-20	0.231	2.4%
3-URG-20	0.219	9.0%
5-URG-20	0.194	3.9%
7-URG-20	0.177	4.3%

In PCC, unit weight is often used as a validation tool for the confirmation of the mix design and air void content. Since the air voids is not measured in the same way for PCPC as it is for PCC, the unit weight is a measure of the workability of a certain mixture. Figure 25 shows the results of the unit weight testing by ASTM C1688.

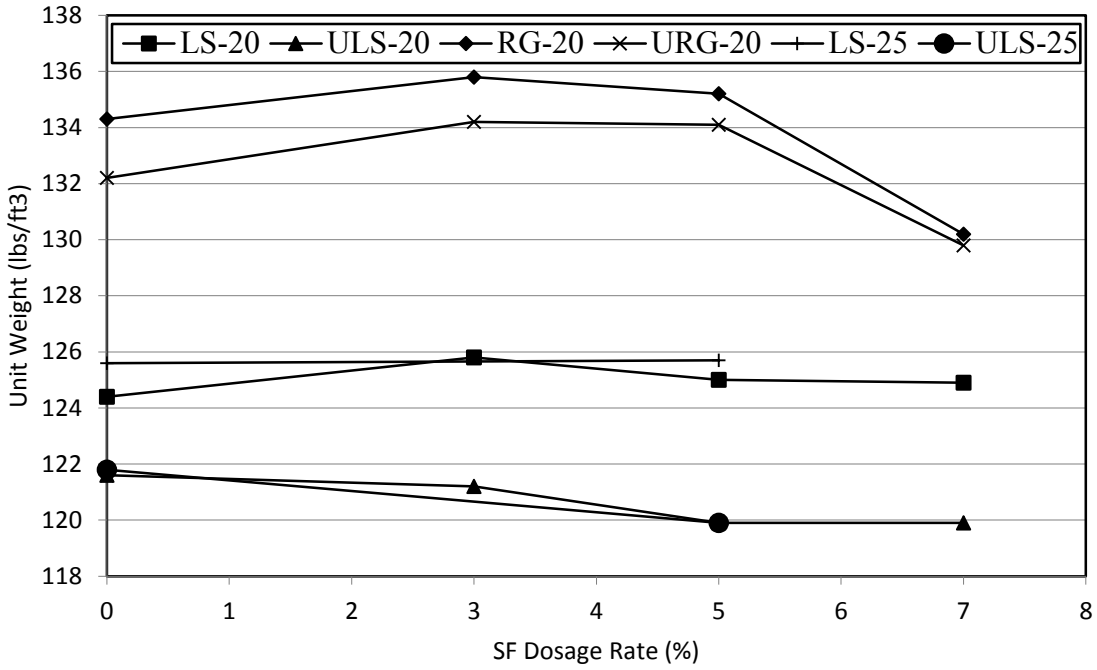

Figure 25 Unit Weight Testing by ASTM C1688

For the RG-20, URG-20, LS-20, and LS-25 samples the unit weight increased for low dosage rates for the 3 percent and 5 percent samples, when compared to the control sample. This is significant because an increase in the unit weight of a sample by ASTM C1688 signifies the mixture compacts more easily and will be more workable. In the RG-20 and URG-20 samples, the unit weight decreased significantly for the 7 percent samples. This was confirmed in the placement and testing of these samples, as these samples took significantly more compaction effort to place at the design void content. It should be noted that ASTM C1688 testing was only conducted once on each mixture. For this reason, it is advised in the "Future Testing" section of this paper to perform additional investigation into the effects of SF on unit weight.

All mix designs described earlier in this paper were all tested for compressive strength at 7 and 28 days. The compressive strength of the samples was taken at 7 and 28

days. The results of the 7-day compressive strength testing results are shown in Figures 26-28 and the 28-day results shown in Figures 29-31.

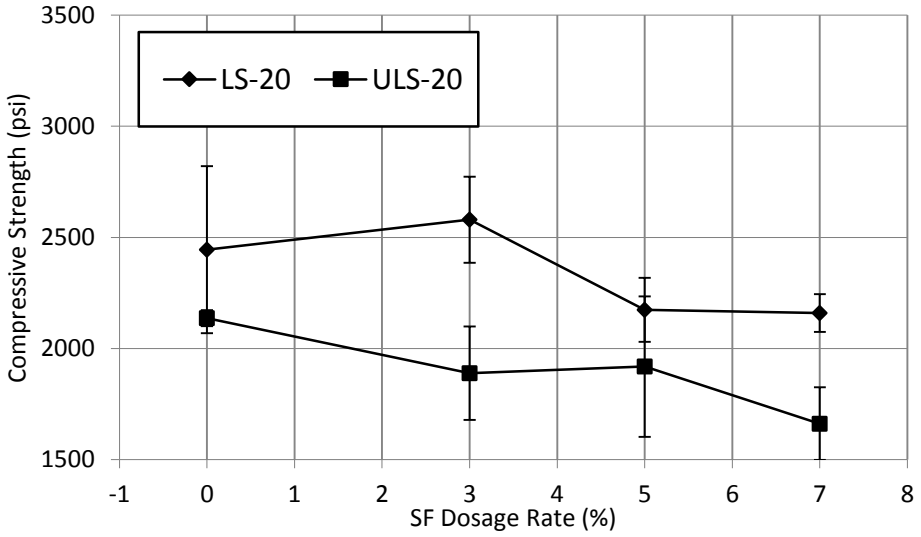

Figure 26 7-day 20-Percent Design Voids Limestone Compressive Strength Values

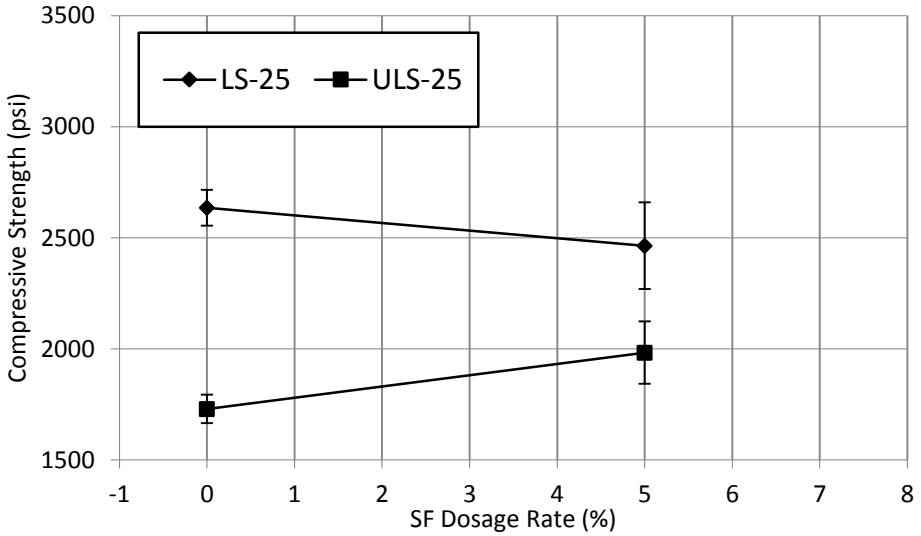

Figure 27 7-day 25-Percent Design Voids Limestone Compressive Strength Values

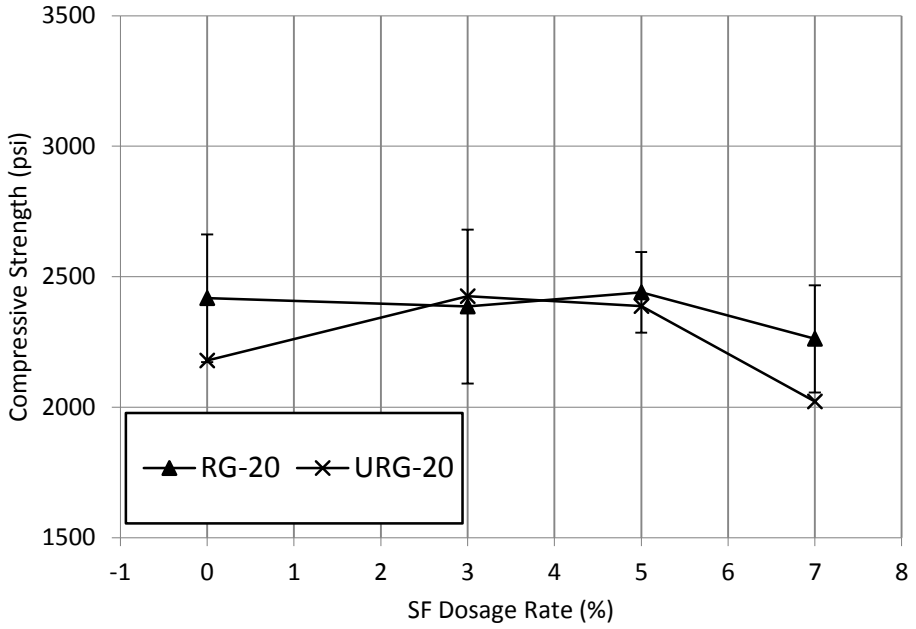

Figure 28 7-day 20 Percent Design Voids River Gravel Compressive Strength Values

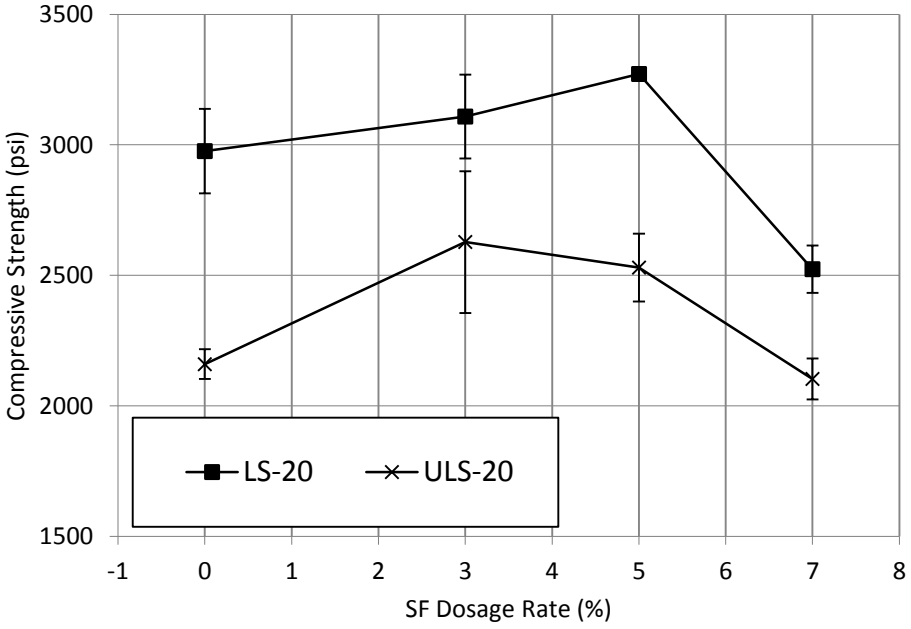

Figure 29 28-day 20-Percent Design Voids Limestone Compressive Strength Values

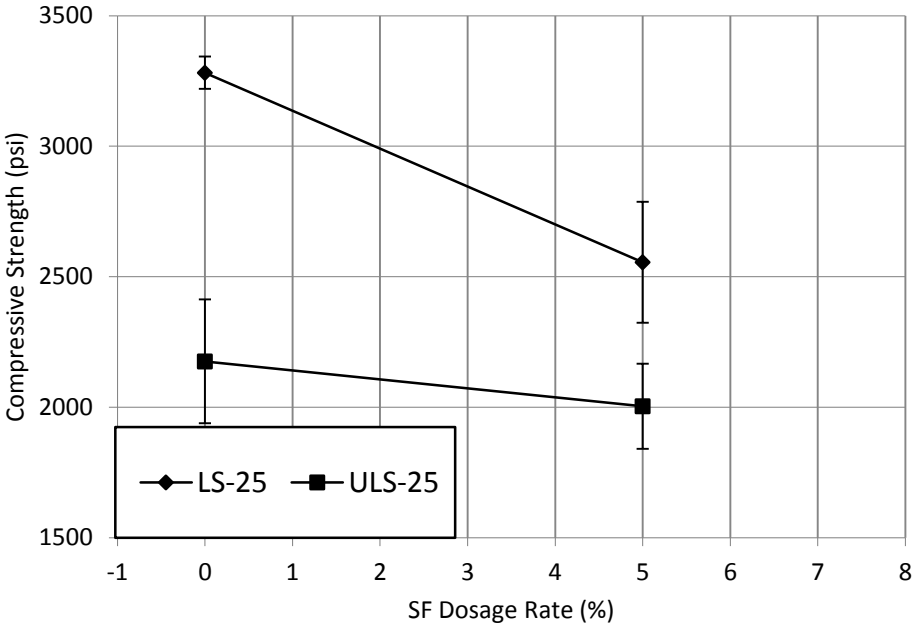

Figure 30 28-day 25-Percent Design Voids Limestone Compressive Strength Values

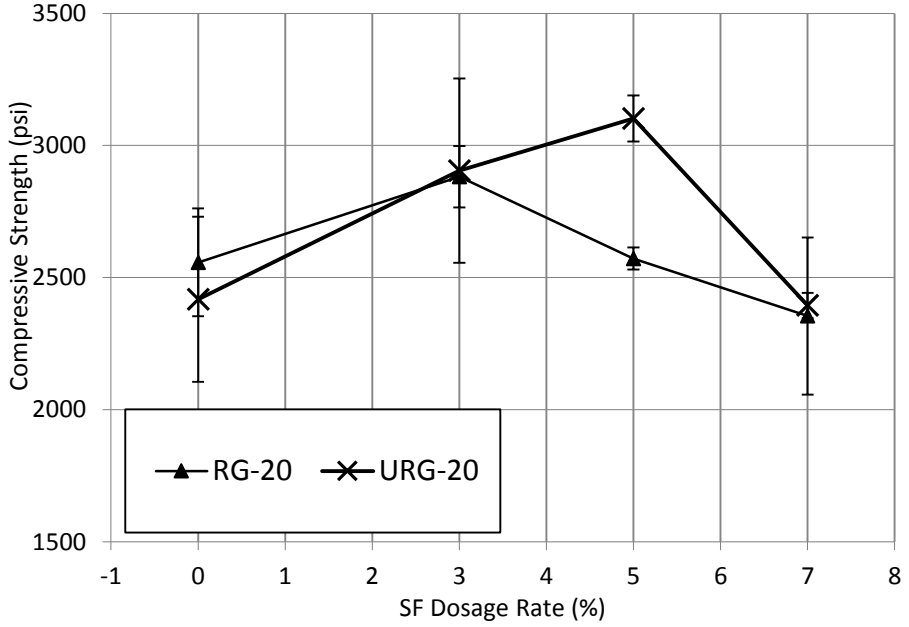

Figure 31 28-day 20-Percent Design Voids River Gravel Compressive Strength Values

The 7-day sample showed highly variable data when comparing the dosage rates. This is likely because of the secondary nature of the pozzolanic reaction. The LS-20 compressive strength increased with a dosage of 3% SF at the 7-day mark, but decreased with a 7% dosage. Although much of the 3% and 5% data is variable at 7-days, one common trend exhibited among all of the sample groups is that the dosage rate of 7% SF is decreases the compressive strength of PCPC when compared to the control sample.

At 28-days, all 20 percent void sample groups showed a higher average compressive strength at 5% dosage when compared to the control mixture. The LS-20, ULS-20, and URG-20 were statistically different at 5%. The samples had p-values of 0.035, 0.011, and 0.022 respectively. Figures 32 and 33 show examples of a typical broken compressive strength specimens with shear and conical modes of failure. All samples were broken according to ASTM C39 (ASTM Standard C39, 2005) exhibited conical, shear, or a combination of the two failure modes.

Figure 32 Typical Shear Mode of Failure After ASTM C39 Testing

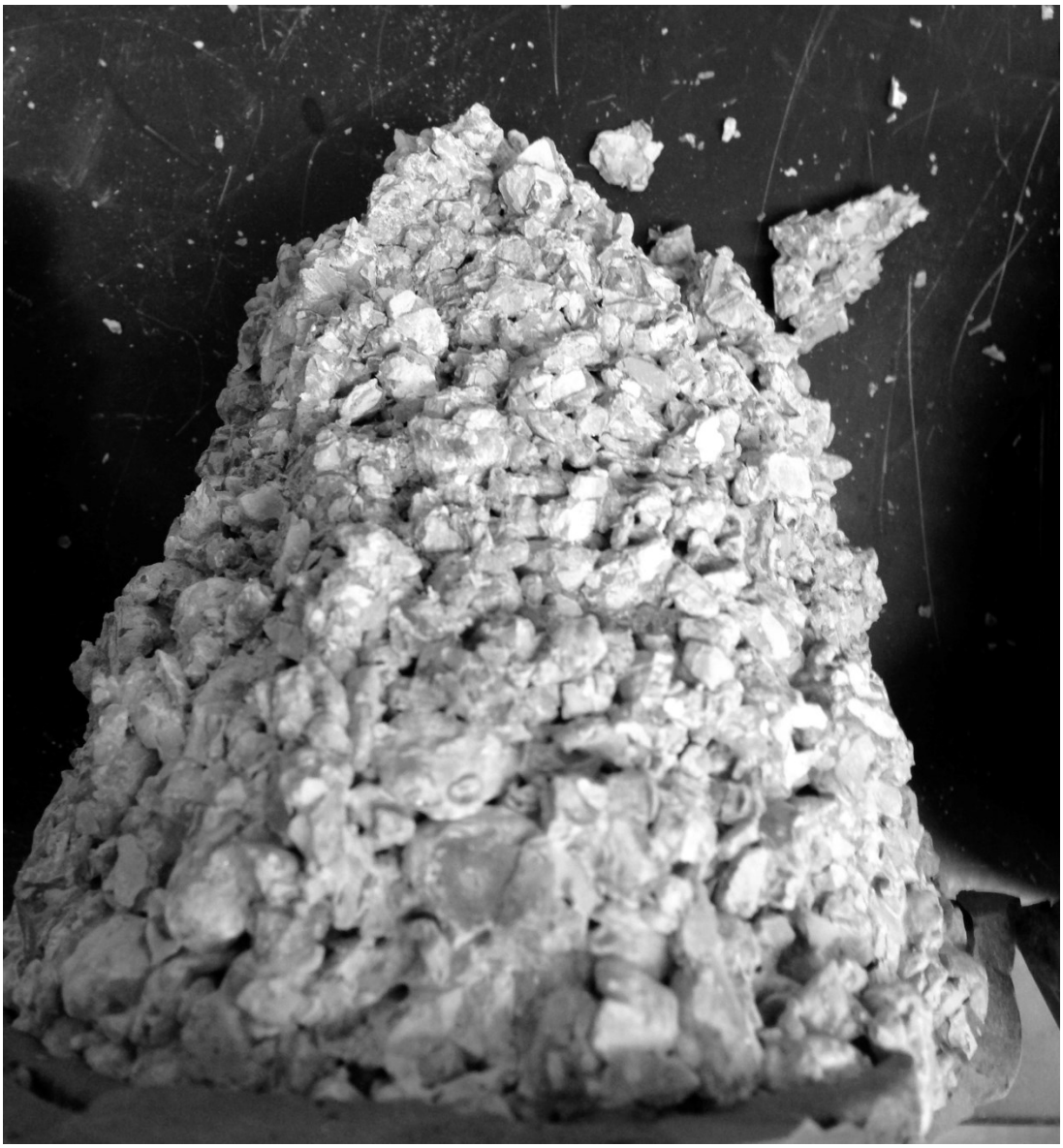

Figure 33 Typical Conical Mode of Failure After ASTM C39 Testing

All 25% samples appeared highly variable with no apparent trends exhibited. The testing for the 25% samples was conducted first, and it was hypothesized this could be due to the variability caused by the increased void content. This hypothesis prompted the testing of the 20% samples after it became apparent the data was highly variable.

It was also noticed that in several of the 7-day unwashed control samples many of the failures in compressive strength testing were due at least in part to aggregate pull out. This phenomenon is a failure in which the bond between the aggregate and the paste does not fully develop due to weaknesses caused by the Interfacial Transition Zone (ITZ). As discussed earlier, SF is especially effective in mitigating the effects of this mode of failure by increasing the density of the paste in the areas immediately surrounding the aggregate. Figure 34 shows an image taken from an optical microscope of a control sample. The area located inside the circle is a region where aggregate pullout occurred. Figure 35 shows a 5% SF sample. In this sample, it can be seen that the sample failed when the aggregate fractured rather than pulling out of the paste of the sample.

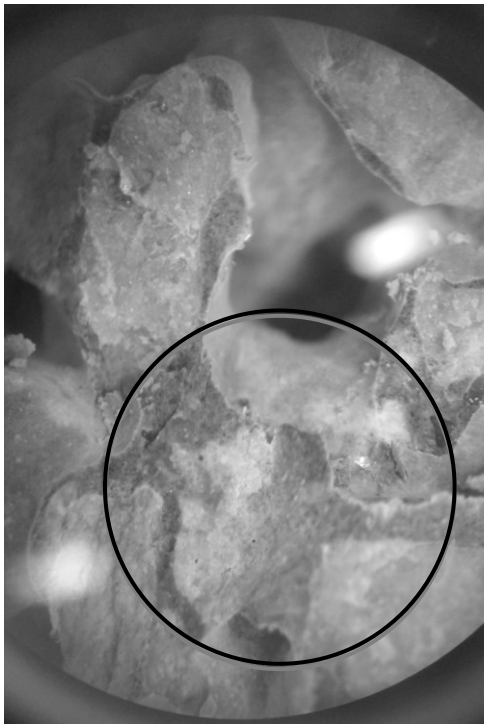

Figure 34 Image of Aggregate Pullout in Control Sample

Figure 35 Aggregate Fracture in 5% SF Sample

The samples were also tested for splitting tensile strength according to ASTM C496 at an age of 28-days. Figure 36 shows the results of the testing and Figure 37 shows a typical broken specimen after undergoing ASTM C496 testing. A summary of all of the compressive strength and tensile strength values for all mixes is shown in Table 17.

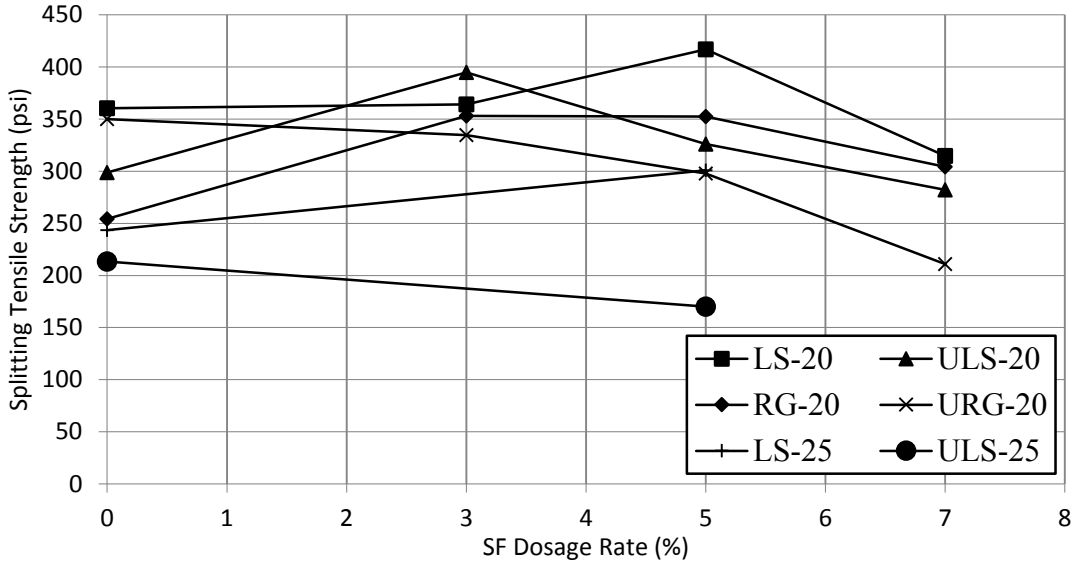

Figure 36 Splitting Tensile Strength by ASTM C496

Figure 37 Typical Failure Mode for Splitting Tensile Strength Testing by ASTM C496

Table 17 Summary of Compressive Strength and Tensile Strength Values

Mix Design	7-Day Compressive Strength		28-Day Compressive Strength		28-Day Splitting Tensile Strength	
	Compressive Strength (psi)	COV (%)	Compressive Strength (psi)	COV (%)	Tensile Strength (psi)	COV (%)
0-LS-25	2635	3.07	3282	1.88	243	7.09
5-LS-25	2464	7.92	2556	9.08	301	7.18
0-ULS-25	1730	3.72	2176	10.89	213	28.90
5-ULS-25	1983	7.08	2004	8.13	170	20.10
0-LS-20	2445	15.38	2976	5.44	360	9.45
3-LS-20	2580	7.51	3109	5.16	364	14.57
5-LS-20	2174	6.60	3272	0.81	417	18.08
7-LS-20	2160	3.93	2524	3.60	315	16.36
0-ULS-20	2137	1.68	2160	2.64	299	22.87
3-ULS-20	1889	11.15	2627	10.32	395	17.78
5-ULS-20	2094	6.38	2530	5.14	326	11.53
7-ULS-20	1662	9.82	2103	3.73	282	10.37
0-RG-20	2418	10.12	2558	7.97	254	15.94
3-RG-20	2386	12.35	2881	4.03	353	5.01
5-RG-20	2440	6.32	2572	1.61	352	9.99
7-RG-20	2262	9.07	2355	12.62	304	5.23
0-URG-20	2179	3.39	2418	12.92	350	20.93
3-URG-20	2425	3.85	2905	12.01	335	17.07
5-URG-20	2387	6.40	3102	2.80	298	6.95
7-URG-20	2022	9.84	2395	2.01	211	5.28

The average tensile strength values for all of the 5% SF samples was greater than that of the control. A larger sample size may be useful in determining the relationship of the splitting tensile strength. Typically, the splitting tensile strength has a relationship to the compressive strength of the samples.

Another test conducted on the samples was the previously mentioned ASTM C944 abrasion testing. In this abrasion test, a rotary cutting wheel was used to grind into the sample for 400 revolutions over a 2 minute period. Rotary abrasion is measured in terms of

average grams lost per sample. Figure 38 and 39 show graphical representations of the results of the testing for limestone and river gravel respectively. The horizontal axis shows the dosage rate of the SF as a percent, and the vertical axis shows the average mass loss from each sample per test. As stated earlier, the scale used met the ASTM specifications in that it is accurate to 0.1 grams.

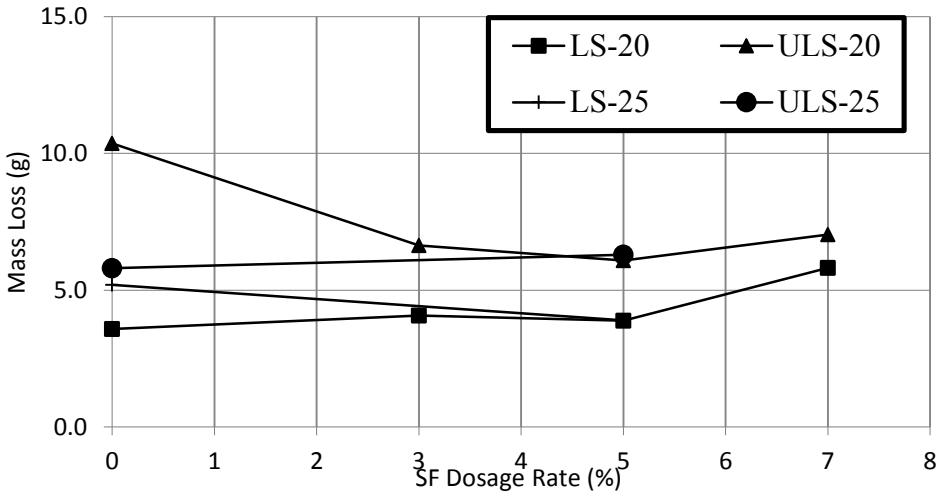

Figure 38 ASTM C944 Limestone Abrasion Testing Data

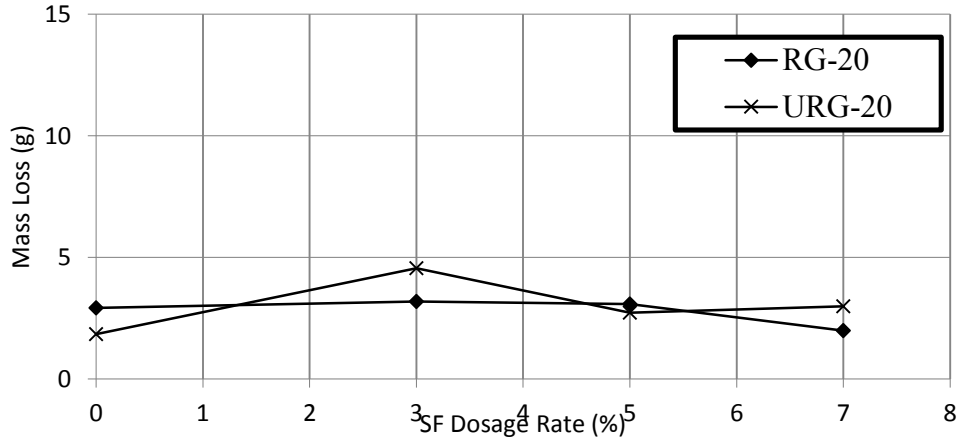

Figure 39 ASTM C944 River Gravel Abrasion Testing Data

The rotary abrasion data shown in Figure 38 exhibited several trends. It was expected that the ULS and URG would have lower strengths and higher abrasion loss than the samples with washed aggregate. This is because the unwashed surface does not allow the paste to develop as strong a bond with the paste. A statistical analysis confirmed this observation for the limestone samples. A comparison between the 0-LS-20 and 0-ULS-20 sample groups yields a p-value of nearly zero, indicating a strong likelihood the samples are from different populations. The testing results from the river gravel sample groups showed no statistically significant trends.

It can be seen that for the samples containing limestone, when SF is added to the mix, the difference between the mass loss decreases when comparing the washed and unwashed samples. In other words, when SF is added, the difference between washed and unwashed limestone becomes less. Table 18 shows a summary of the data comparison used to come to this conclusion. This testing indicated that although it still increases the abrasion resistance of PCPC to wash the aggregate, SF decreases the amount of additional raveling caused by dirty aggregate.

Table 18 Comparison of Mass Loss between Washed and Unwashed Samples

Mix Comparison	**Average Difference Between Samples (g)**
0-LS-20 compared to 0-ULS-20	6.78
3-LS-20 compared to 3-ULS-20	2.25
5-LS-20 compared to 5-ULS-20	1.93
7-LS-20 compared to 7-ULS-20	0.65

Although SF appeared to have a positive effect on the bond strength of the paste to the aggregate in mitigating abrasion in dirty aggregate when comparing similar dosage rates,

the effect of the dosage rate varied between tested samples. The samples appeared to have at best a neutral effect when comparing samples with the same aggregate treatment but varying dosage rates. It was visually apparent when comparing samples that the abrasion samples with high SF contents tended to have more spalling than the control samples in ASTM C944. Figures 40 through 43 show the abrasion samples for the LS-20 sample group. Figure 44 shows a close-up of 7-LS-20.

Figure 40 0-LS-20 ASTM C944 Abrasion Sample

Figure 41 3-LS-20 ASTM C944 Abrasion Sample

Figure 42 5-LS-20 ASTM C944 Abrasion Sample

Figure 43 7-LS-20 ASTM C944 Abrasion Sample

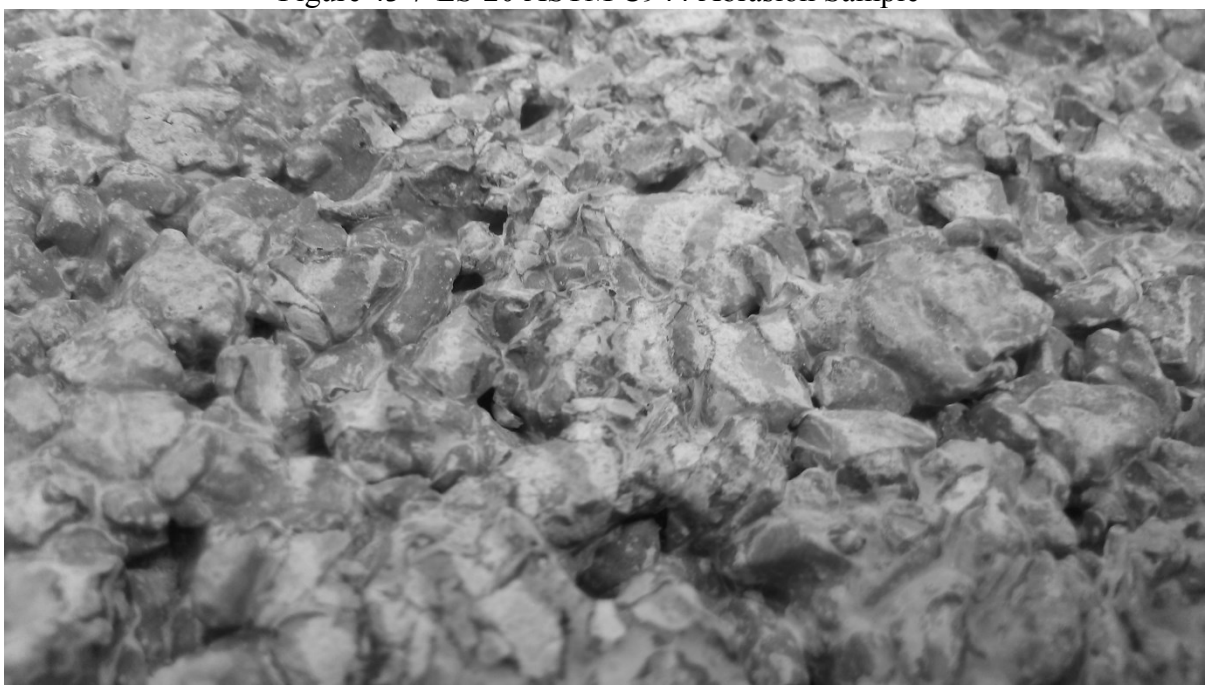

Figure 44 Abrasion Marks Left by Rotary Cutting Wheel on Sample

As described earlier in the testing methods portion of this paper, an impact form of abrasion testing was conducted on several of the PCPC samples according to ASTM C1747. The results of this testing are shown in Figure 45, and are reported as percent mass lost. This test requires three samples to perform. The samples, however, are mixed together in the rotating drum, so there is no way to distinguish the samples from each other. For this reason, despite testing in triplicate, only an average mass loss can be calculated for the samples and no coefficient of variance. For this reason, apparent trends can be seen, but a statistical analysis is not possible.

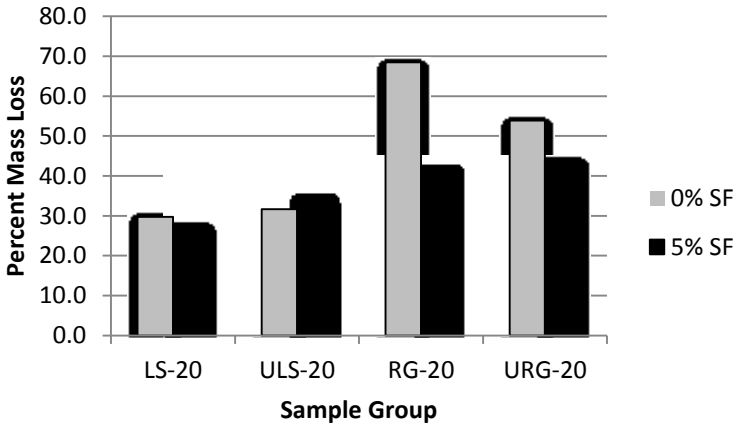

Figure 45 Impact Abrasion Testing Results by ASTM C1747

In analyzing the data for impact abrasion, several apparent trends can be identified. The first, and probably most apparent, is that the river gravel appears to have an increased susceptibility to raveling when compared to the limestone. This was expected, since the river gravel had lower angularity than the limestone samples which make the bond between paste and aggregate weaker. The 0-RG-20 sample exhibited an exceptionally high mass loss. This contradicted the trends exhibited in other testing of better performance in the unwashed aggregate than the washed aggregate.

Another trend seen in the impact abrasion testing was the decrease in mass loss for the samples containing SF, when compared to the control with the exception of the ULS-20 samples. The SF appeared to have a greater impact on the mitigation of raveling in the samples utilizing river gravel. Figures 46 and 47 show the samples after undergoing testing for the LS and RG mixtures respectively.

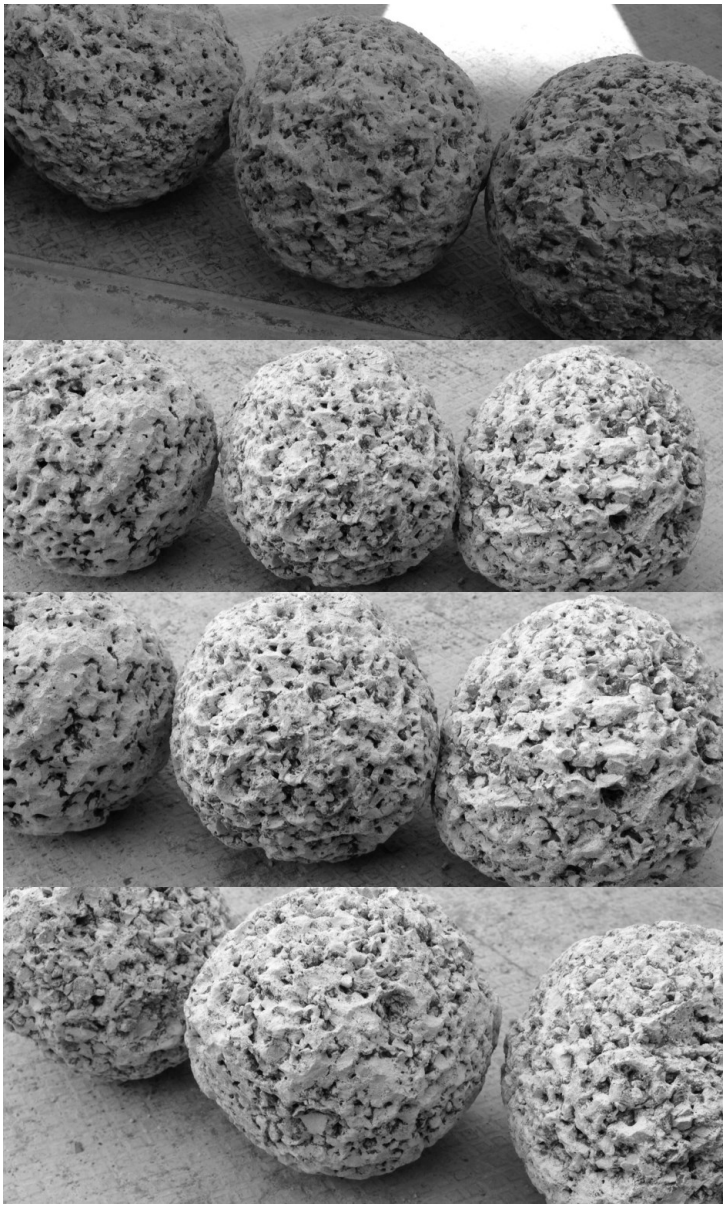

Figure 46 Limestone Samples After Impact Abrasion by ASTM C1747 from Top to Bottom 0-LS-20, 5-LS-20, 0-ULS-20, 5-ULS-20

Figure 47 River Gravel Samples After Impact Abrasion by ASTM C1747 from Top to Bottom 0-RG-20, 5-RG-20, 0-URG-20, 5-URG-20

Although impact and rotary abrasion both test a PCPC mix design for susceptibility for raveling, often results are quite different. An attempt was made to correlate the two forms of abrasion testing, and can be seen in Figure 48. For the sample sizes tested, no trend was apparent.

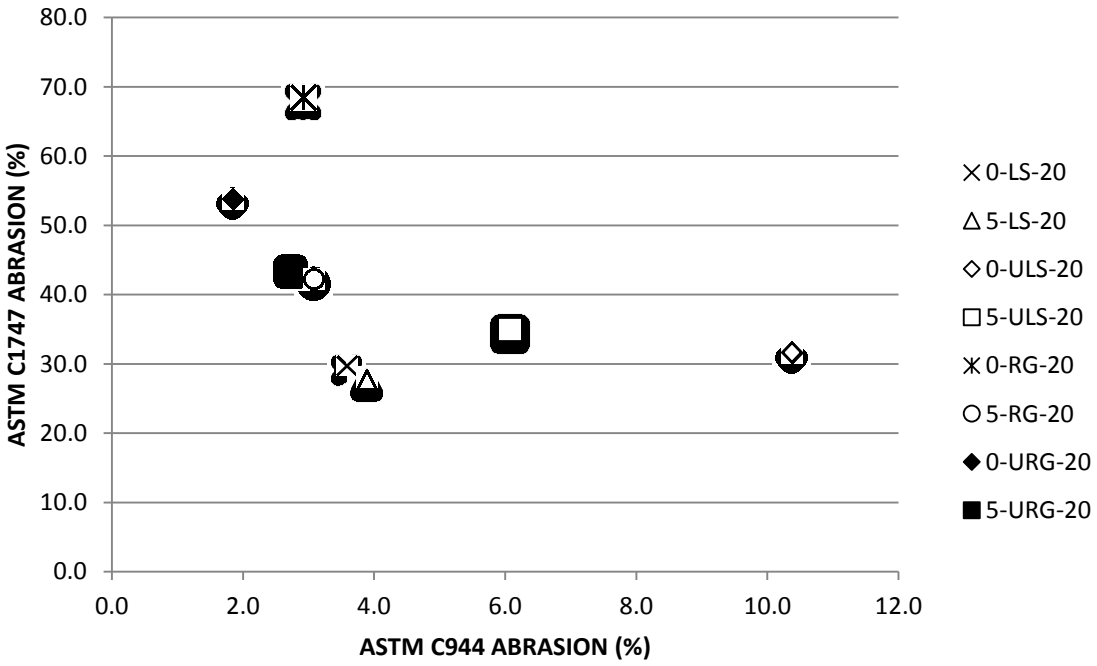

Figure 48 Impact Abrasion by ASTM C1747 Relationship with Rotary Abrasion by ASTM C944

Although abrasion testing is an indicator of the ability of a PCPC mix to withstand the forces which often cause raveling, another important durability test is freeze-thaw testing. PCPC under ideal conditions would never be fully submersed under freezing conditions, but if it becomes cogged it is important to understand how freezing and thawing would affect the mix. Using ASTM C666, freeze thaw testing was conducted. Figure 49 depicts the results of

the control testing for the 25 percent samples, and shows that washing the aggregate makes a difference in the freeze thaw durability.

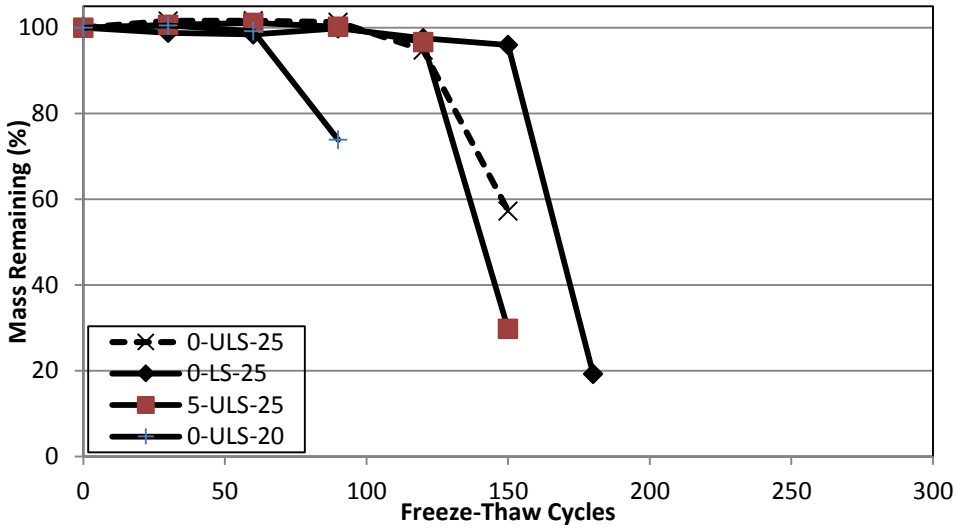

Figure 49 Freeze-Thaw Testing for Control Samples

As found in other phases of testing, the washing of the aggregate made a significant improvement in the performance of the PCPC. The washed control sample failed at an average of 180 cycles whereas the unwashed sample failed at an average of 150 cycles. Figures 50- 53 show examples of the before and after of the 0-LS-25 and 5-LS-25 test groups. Figures 54-57 show examples of the before and after of the 0-ULS-25 and 5-ULS-25 sample groups. Figure 58 shows a comparison of the control and SF samples for the unwashed sample groups.

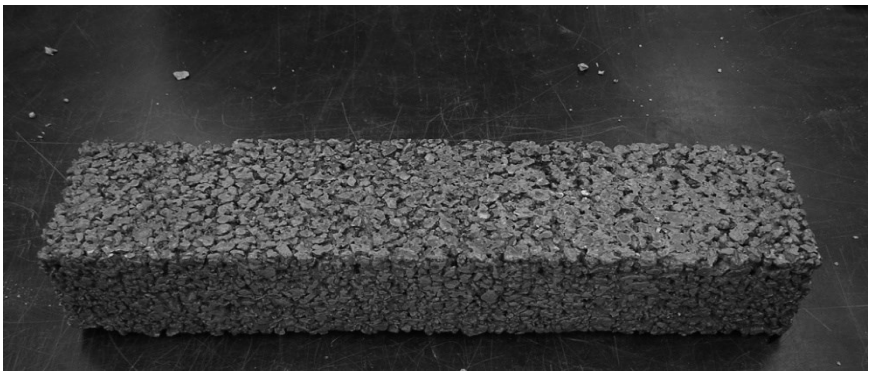

Figure 50 0-LS-25 Sample Before ASTM C666 Testing

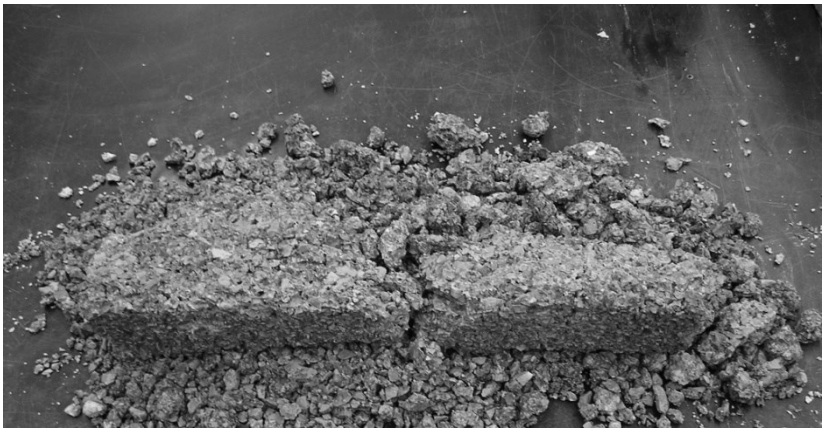

Figure 51 0-LS-25 After ASTM C666 Testing

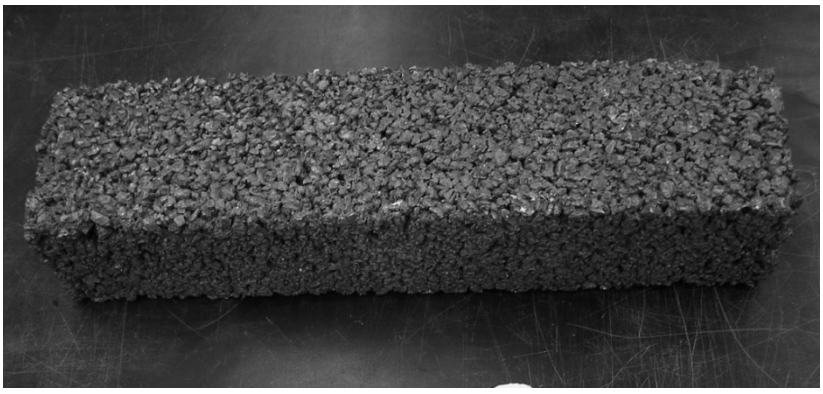

Figure 52 5-LS-25 Before ASTM C666 Testing

Figure 53 5-LS-25 After ASTM C666 Testing

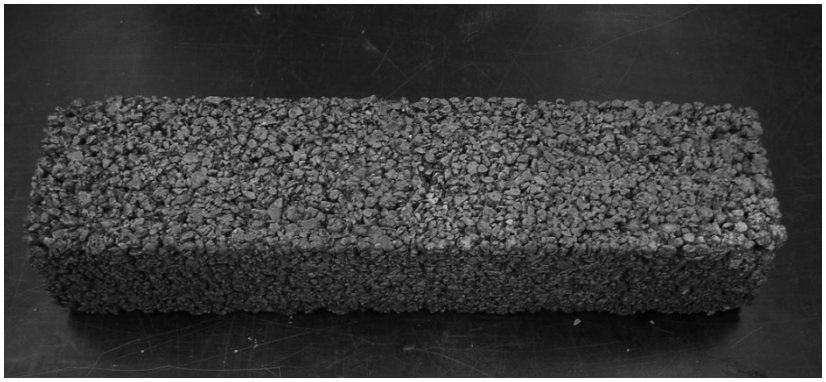

Figure 54 0-ULS-25 Before ASTM C666 Testing

Figure 55 0-ULS-25 After ASTM C666 Testing

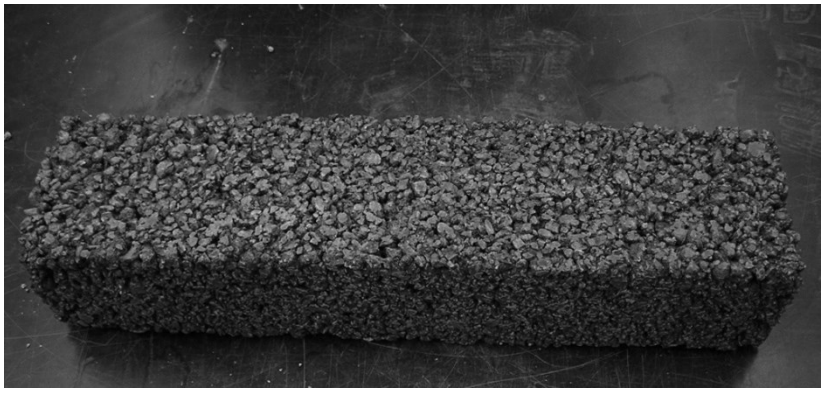

Figure 56 5-ULS-25 Before ASTM C666 Testing

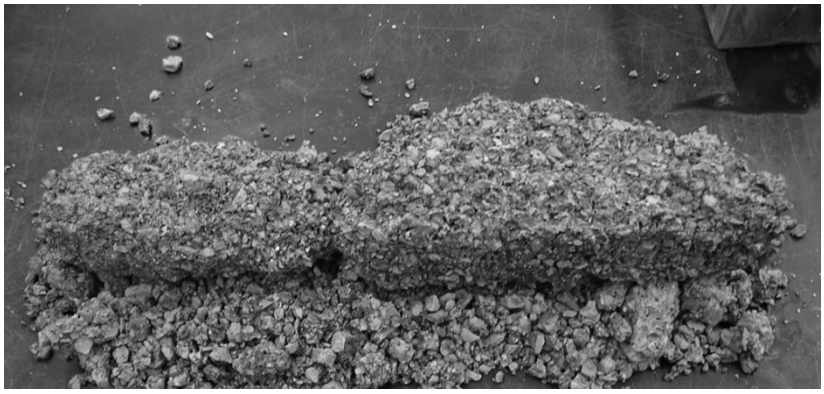

Figure 57 5-ULS-25 After ASTM C666 Testing

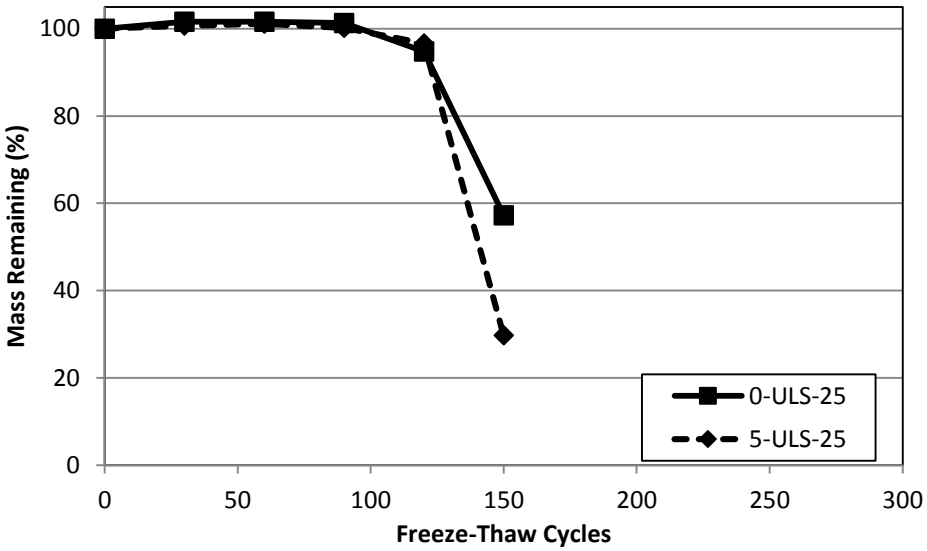

Figure 58 Freeze-Thaw Results Comparing Unwashed Samples

Figure 58 showed that the failure of both of the samples occurred at an average of 150 freeze-thaw cycles. However, SF did not improve the amount of mass loss at the time of failure for the specimens. At 150 cycles, the SF samples had lost approximately twice as much as the control samples. The SF samples had an average of 29 percent of their original mass remaining, whereas the control samples had an average of 57 percent. While Figure 49 reiterated the importance of washing the aggregate in the control sample, Figure 59 shows how the SF affected the need to wash the aggregate.

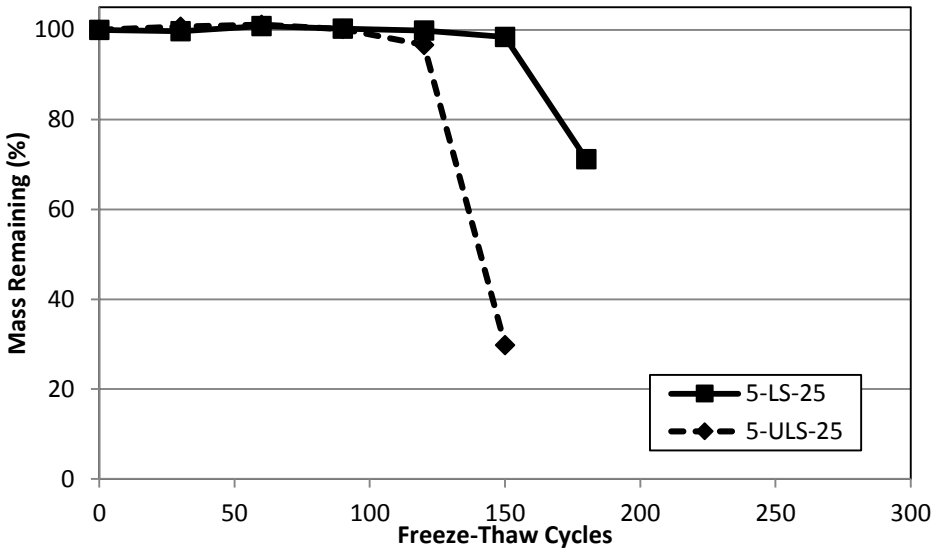

Figure 59 Freeze-Thaw Results Comparing Washed and Unwashed SF Samples

The washed sample showed a significant increase in the number of cycles before failure, lasting a total of 180 cycles compared to the unwashed sample lasting 150 cycles. Similar to the control samples, Figure 59 shows that the washed sample failed at 180 cycles and the unwashed sample failed at 150 cycles.

The difference shown in this test is that the washed sample had a much higher mass remaining at 180 cycles. Figure 60 depicts this relationship.

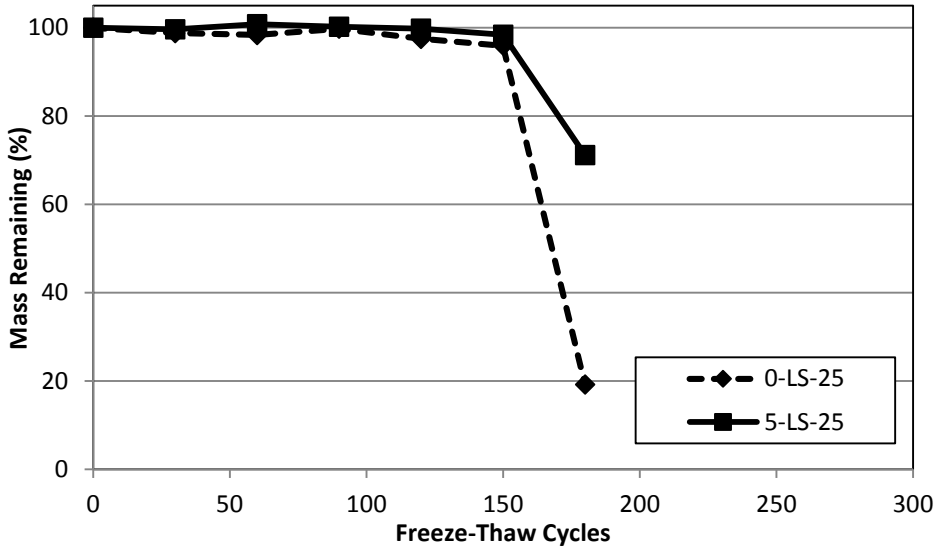

Figure 60 Freeze Thaw Testing Results Comparing Washed Samples

Figure 60 shows that while both the washed SF sample and washed control sample fail at 180 cycles, the remaining mass is much higher for the sample containing SF. The sample containing SF retains nearly 70 percent of its original mass whereas the control retains around 20 percent.

A comparison of the washed limestone samples at both 20 percent and 25 percent is shown in Figure 61. The results of the Freeze-Thaw testing suggested that the 5 percent SF sample had the best durability. The 25 percent sample with SF performed better than the control at the same voids, but the 20 percent sample with SF failed at a lower number of cycles than did the 20 percent control.

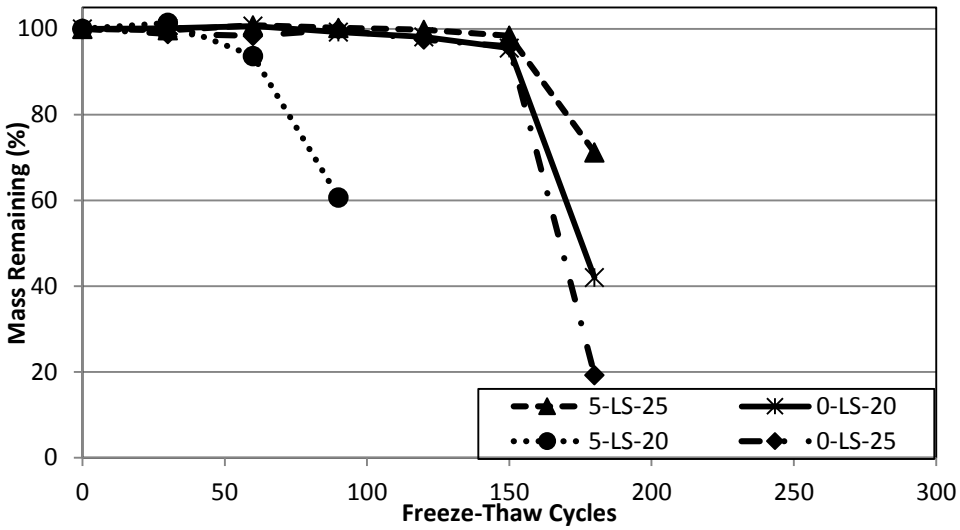

Figure 61 Freeze-Thaw Testing Results Comparing Washed Limestone Samples at 20 and 25 Percent Voids

Figure 62 shows a comparison of the unwashed limestone samples. The result of this comparison shows the 25 percent unwashed sample with SF as having the second best durability when comparing all unwashed limestone samples.

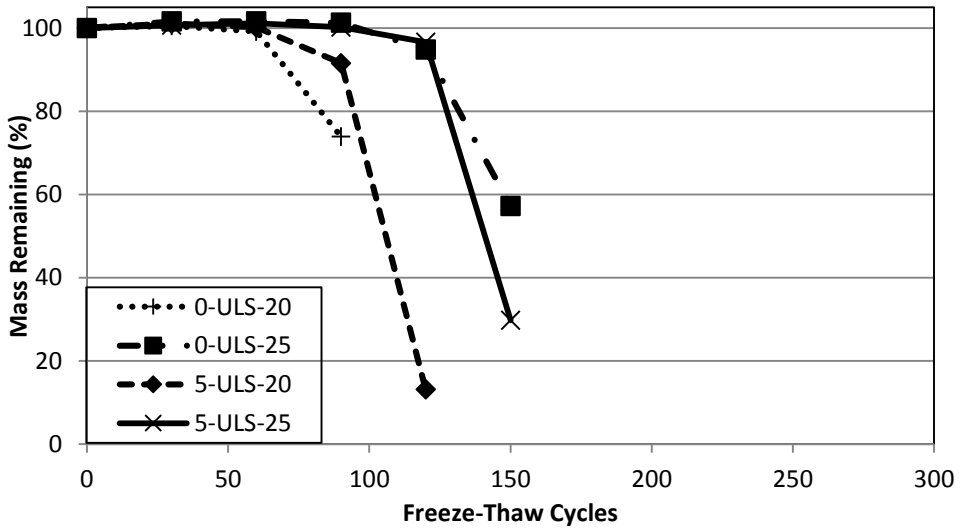

Figure 62 Freeze-Thaw Testing Results Comparing Unwashed Limestone Samples at 20 and 25 Percent Voids

Both the washed and unwashed limestone samples seem to suggest the 25 percent mixture is more durable. This is likely because the 25 percent void limestone samples have a structure in which the voids are more connected, allowing more paths for the water to expand as the water freezes. Although results varied when comparing groups, it also appeared that SF generally increased the durability of the mixtures containing limestone.

The river gravel results varied significantly from the limestone samples. It did not appear that SF greatly increased the durability of the PCPC containing river gravel. Figure 63 shows the results of this testing.

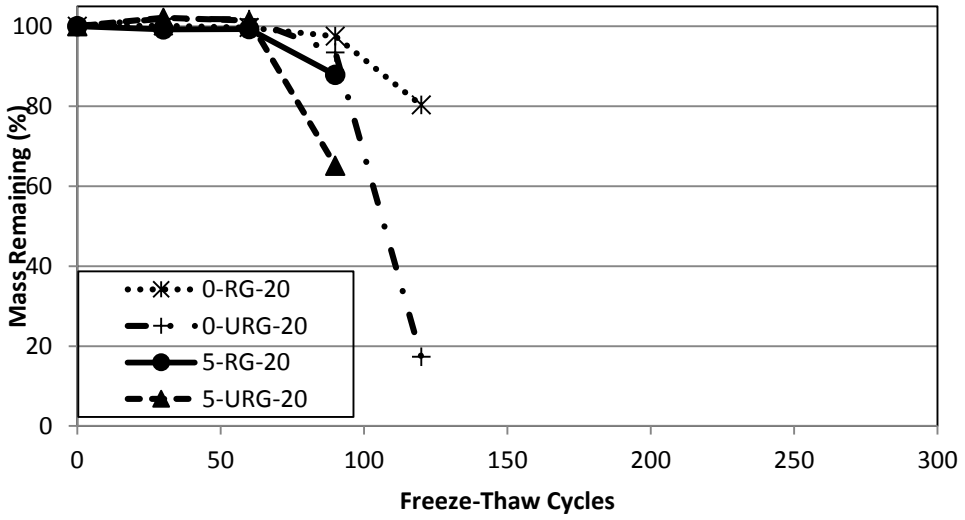

Figure 63 Freeze-Thaw Testing Results Comparing Washed and Unwashed River Gravel Samples

CHAPTER 8

CONCLUSIONS

An ever increasing need is presenting itself worldwide to handle stormwater in an economically and environmentally sustainable way. Although Portland Cement Pervious Concrete (PCPC) is one such tool that has been used, it is often subject to durability and strength issues. In this paper, Silica Fume (SF) was used in a variety of mixes to determine its effect on the performance of PCPC.

Testing of the PCPC included two main phases. The first phase was a rheological study to determine the effects of SF on the viscosity of the paste. The second phase consisted of tests on PCPC at several dosage rates and void contents. This phase of testing focused on the quality control, workability, strength, and durability of the concrete.

A large portion of this phase of testing consisted of evaluating mixes to determine the appropriate mix to attain 20 percent voids and 25 percent voids. If the concrete was not batched at the same void content, comparisons of mixes would be difficult, since the void content has such a drastic effect of the properties of hardened concrete. In addition to measuring the void content of the mixes, permeability testing was conducted on the 20 percent mixes.

The test conducted to determine the workability of the PCPC was the unit weight test. Although in PCC unit weight is utilized more as a verification that the correct materials were batched into the mix, unit weight in PCPC is used as a measure of workability.

The tests for strength included compressive strength testing at 7 days, 28 days, and splitting tensile testing at 28 days. In addition to evaluating the PCPC mixes for strength,

the mixes were also evaluated for durability by testing the rotary abrasion, impact abrasion, and freeze-thaw durability.

After conducting these tests and analyzing the results, several conclusions can be made regarding the use of silica fume as a supplementary cementing material for use in Portland cement pervious concrete:

1. Cement paste containing silica fume does have a non-linear relationship between stress and strain, and exhibits shear thinning tendencies. This would tend to indicate that silica fume would mix better at a higher shear rate, and could mean that in real world applications a faster mixing speed would result in a better mix for mixes containing silica fume.
2. In cement paste, silica fume dosage is most workable at just over 5 percent silica fume dosage by weight. The viscosity and yield stress increase slightly from 0 to 5 percent silica fume dosage rate, then begin to increase dramatically past 5 percent.
3. PCPC mixes containing silica fume at the 3 to 5 percent range tended to have a higher compressive and splitting tensile strength than the control samples. Most mixes with silica fume dosage rates of 7 percent exhibited a decrease in compressive strength.
4. Mixes containing silica fume improved the viscosity of the paste when mixed at hot weather conditions. Although it should be investigated further, silica fume may be a useful tool in pervious mixes that occur in areas with high ambient air temperatures and low humidity.

5. The mixes containing silica fume appeared to exhibit a stronger bond to the aggregate than the control mixes. This was confirmed visually in the apparent reduction of aggregate pull out, especially in the river gravel samples, and in the strength exhibited in the samples containing silica fume.
6. Since mixes were batched by density, permeability and void content was not affected by the addition of silica fume. PCPC mixes containing silica fume should be placed in such a way that the mass of the concrete is known for the given volume being filled, and the compaction effort adjusted accordingly. Since silica fume affects the workability of concrete, if the same compaction effort is not calibrated to the mix being used, higher or lower voids and permeability than designed could result.
7. Results of ASTM C1747 showed that river gravel was more susceptible to raveling due to impact abrasion deterioration when compared to limestone. Results of ASTM C944 showed that limestone mixes were more susceptible to surface abrasion when compared to limestone.
8. The addition of silica fume had a greater effect on unwashed limestone than it did on washed limestone. As a result, silica fume reduced the importance of washing the limestone aggregate.
9. Rotary abrasion, impact abrasion, splitting tensile strength, and compressive strength testing results confirmed the idea that the washing of aggregate being utilized improves the performance of concrete. The bond between the aggregate and paste is especially important in PCPC where the

surface area in which the two interact is less than in PCC, and clean aggregate appears to be a key factor in achieving a strong bond.

10. Applying ultrasound to a mortar mixture with while hand mixing did not have an effect on compressive strength of the samples. More testing may be warranted on mixes with differing levels of workability and mixing techniques to determine if ultrasound may still be useful during the mixing phase.

11. Different freeze-thaw tests yielded conflicting results. Testing as a whole for ASTM C666 was inconclusive. As noted in the next chapter, additional freeze-thaw testing is needed to obtain statistically significant results.

CHAPTER 9

FUTURE TESTING

In addition to the testing completed in this study, additional testing would be recommended by the author. Although the testing was done in triplicate, it would be suggested that additional testing be conducted for impact abrasion. Since all three samples are placed in the LA abrasion apparatus at the same time, it is impossible to gain a COV to determine more advanced statistics. In addition, it would be worthwhile to conduct additional testing on more samples of various void content to determine any effects on abrasion the silica fume may have at different void contents.

Additional testing should also be conducted on unit weight testing. Since the unit weight in PCPC is often used as a measure of the workability of the cement, more samples at a more widespread dosage rate would be useful in determining a more accurate relationship between silica fume and PCPC workability.

Although testing has previously been conducted on silica fume in traditional concrete and mortar, it may be beneficial to perform rounds of testing in which mortar cubes are mixed, placed, and tested at a PCPC paste design. Being able to correlate the properties of mortar to the properties of PCPC may save both time and money in determining an optimal mix design. More testing should also be conducted on the ultrasound mixing techniques to determine if there is a configuration that allows the silica fume particles to deflocculate.

More testing should be conducted using various mixing times. Rheology testing allowed testing at many different times in a silica fume and cement paste, but time and money factors limited the ability to conduct multiple trials on the effects of mixing time on

PCPC. Testing the unit weight at different mixing times would yield good insight on how the workability of the mix reacts to different mixing times.

In addition to additional laboratory testing, a field test panel placed with a 5 percent dosage rate of silica fume may be beneficial. Often times, samples poured in the field reveal additional issues that laboratory testing cannot predict.

REFERENCES

1. American Concrete Institute. (1996). *ACI 234R-96: Guide for the Use of Silica Fume in Concrete.* American Concrete Institute.

2. American Society of Civil Engineers. (2014). *Wastewater*. (A. S. Engineers, Producer) Retrieved from 2013 Report Card For America's Infrastructure: http://www.infrastructurereportcard.org/a/#p/wastewater/overview

3. ASTM Standard C109. (2013). Standard Test Method for Compressive Strength of Hydraulic Cement Mortars (Using 2-in. or [50-mm] Cube Specimens). *ASTM International*, DOI: 10.1520/C0109_C0109M, 2013, www.astm.org.

4. ASTM Standard C1747. (2011). Standard Test Method for Determining Potential Resistance to Degradation of Pervious Concrete by Impact and Abrasion. *ASTM International, West Conshohocken, PA*, DOI: 10.1520/C1747_C1747M-11, 2011, www.astm.org.

5. ASTM Standard C1754. (2012). Standard Test Method for Density and Void Content of Hardened Pervious Concrete. *ASTM International, West Conshohocken, PA*, DOI: 10.1520/C1754_C1754M-12, 2012, www.astm.org.

6. ASTM Standard C39. (2005). Standard Test Method for Compressive Strength of Cylindrical Concrete Specimens. *ASTM International, West Conshohocken, PA*, 2005, DOI: 10.1520/C0039_C0039M-05, www.astm.org. Retrieved from astm.org

7. ASTM Standard C496. (2004). Standard Test Method for Splitting Tensile Strength of Cylindrical Concrete Specimens. *ASTM International, West Conshohocken, PA*, DOI: 10.1520/C0496_C0496M-04E01, 2004, www.astm.org.

8. ASTM Standard C666. (2008). Standard Test Method for Resistance of Concrete to Rapid Freezing and Thawing. *ASTM International*, DOI: 10.1520/C0666_C0666M-03R08, 2008, www.astm.org.

9. ASTM Standard C944. (1999). Standard Test Method for Abrasion Resistance of Concrete or Mortar Surfaces by the Rotating-Cutter Method. *ASTM International*, DOI: 10.1520/C0944-99, 2005, www.astm.org.

10. Bingham, E. C. (1922). *Fluidity and Plasticity.* New York: McGraw Hill Book Company.

11. Bohni, H. (2005). *Corrosion in Reinforced Concrete Structures.* CRC Press.

12. Enviromental Protection Agency. (2012, November 5). *Stormwater Management Best Practices*. Retrieved from Enviromental Protection Agency: http://www.epa.gov/oaintrnt/stormwater/best_practices.htm#permeablepavement

13. Federation Internationale de la Precontrainte. Commision on Concrete. (1988). *Condensed Silica Fume in Concrete.* London.

14. Ferraris, C. F., Obla, K. H., & Hill, R. (2001). The influence of mineral admixtures on the rheology of cement paste and concrete. *Cement and Concrete Research, 31*, 245-255.

15. Herschel, W., & Bulkley, R. (1926). Konsistenzmessungen von Gummi-Benzollösungen. *Kolloid Zeitschrift , 39*, 291-300.

16. Holland, T. C. (2005). *Silica Fume User's Manual.* Silica Fume Association & Federal Highway Administration. Springfield, VA: National Technical Information Service.

17. Lange, F., Mortel, H., & Rudert, V. (1997). Dense packing of cement pastes and resulting consequences on mortar properties. *Cement and Concrete Research, 27*(10), 1481-1488.

18. Lian, C., & Zhuge, Y. (2010). Optimum mix design of enhanced permeable concrete – An experimental investigation. *Construction and Building Materials, 24*, 2664-2671.

19. Limbachiya, M., Meddah, M. S., & Ouchagour, Y. (2012, January-February). Performance of Portland/Silica Fume Cement Concrete Produced with Recycled Concrete Aggregate. *ACI Materials Journal, 109*(1), 91-100.

20. Lootens, D., Hebraud, P., Lecolier, E., & Van Damme, H. (2004). Gelation, Shear-Thinning and Shear-Thickening in Cement Slurries. *Oil & Gas Science & Technology, 59*(1), 31-40.

21. Lu, G., & Wang, K. (2011). Theoretical and experimental study on shear behavior of fresh mortar. *Cement & Concrete Composites, 33*, 319-327.

22. McCormac, J. C., & Brown, R. H. (2009). *Design of Reinforced Concrete.* Hoboken, NJ: John Wiley & Sons, Inc.

23. Rashad, A. M., Seleem, H. E.-D., & Shaheen, A. F. (2014). Effect of Silica Fume and Slag on Compressive Strength and Abrasion Resistance of HVFA Concrete. *International Journal of Concrete Structures and Materials, 8*(1), 69-81.

24. United States Conference of Mayors. (2005). *Impact of Unfunded Federal Mandates and Cost Chifts on U.S. Cities: A Preliminary Report on Costs in 59 Cities.* The United States Conference of Mayors. Washington, D.C.: City Policy Associates.

25. Vikan, H., Justnes, H., Winnefeld, F., & Figi, R. (2007). Correlating cement characteristics with rheology of paste. *Concrete & Cement Research, 37*, 1502-1511.

26. Wu, H., Huang, B., Shu, X., & Dong, Q. (2011). Labratory Evaluation of Abrasion Resistance of Portland Cement Pervious Concrete. *Journal of Materials, 23*(5), 697-702.

27. Yang, J., & Jiang, G. (2003). Experimental study on properties of pervious concrete pavement materials. *Cement and Concrete Research , 33*, 381-386.

VITA

Daniel Allen Mann was born July 25th 1990 in Anchorage, Alaska. He attended Washington High School in Washington, Missouri where he participated in track & field, cross country, and multiple other organizations. Dan attended Missouri University of Science and Technology before transferring to the University of Missouri-Kansas City in the fall of 2009. Dan was varsity student-athlete and team captain of the UMKC Kangaroos in Track & Field and Cross Country holding a school record and multiple all-time top 5 performances. He was also a member of several organizations including Tau Beta Pi, Chi Epsilon, and the American Society of Civil Engineers. Dan graduated Cum Laude in 2012 with a Bachelor of Science in Civil Engineering from UMKC before returning to work towards his Masters of Science the following semester. Dan worked during his time as a graduate student in the lab of Dr. John T. Kevern researching pervious pavement, and currently works for Olsson Associates on the Transportation Engineering team.